RAMAN SPECTROSCOPY STUDY OF RARE-

EARTH DOPED SILICATE GLASSES:

MECHANISM UNDERLYING

HOLOGRAPHIC GRATING

FORMATION

By

ZHANDOS UTEGULOV
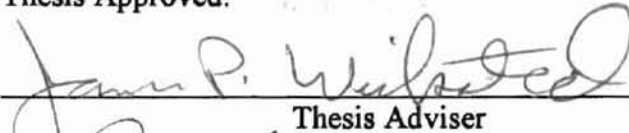
Bachelor of Science
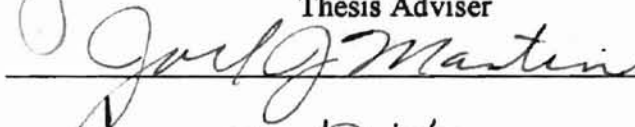
Kazak State National University

Almaty, Kazakstan

1996

Submitted to the faculty of the
Graduate College of the
Oklahoma State University
in partial fulfillment of
the requirements for
the Degree of
MASTER OF SCIENCE
May, 1999

RAMAN SPECTROSCOPY STUDY OF RARE-

EARTH DOPED SILICATE GLASSES:
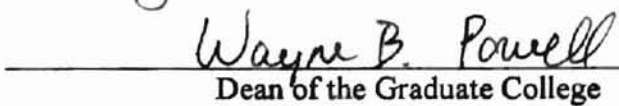
MECHANISM UNDERLYING

HOLOGRAPHIC GRATING

FORMATION

Thesis Approved:

_____
Thesis Adviser

_____

_____

_____
Dean of the Graduate College

ACKNOWLEDGMENTS

TABLE OF CONTENT

LIST OF FIGURES

CHAPTER I

INTRODUCTION

Holographic recording media utilizing the effect of grating formation can be used in optical signal processing applications as the substrates for optical signal transfer and memory elements. Glasses with photorefractive responses have recently been utilized as the materials for holographic media (Behrens *et al.*, (1990)). Glass media avoid many of the difficulties associated with the manufacture of single crystals and thin films. They are easily molded into configurations needed for efficient device operation and can be economically mass-produced. The photorefractive compositions include glasses that are mechanically robust and tolerant to environmental changes. When probed by radiation of sufficiently long wavelength, glass appears homogeneous and locally anisotropic due to its amorphous structure. Because of these factors, systems and products manufactured from glass are commercially more attractive than those requiring single crystals for their implementation.

Of particular interest are rare-earth activated glasses which support photorefractive gratings by writing into excited states with strong nonradiative decay channels. Persistent gratings formed in rare earth doped silicate glasses are shown to be stable photorefractive materials. The extreme stability of the persistent gratings in these glasses makes them competitive candidates for optical demultiplexers, filters and ROM – memories. There is great potential for forming these glass-based as

integrated fiber optic devices. In their present state of development, the grating strengths in these glasses are still somewhat weaker than those of the best crystalline photorefractive materials, but there is evidence that these can be improved by optimization of the composition and processing parameters.

Laser induced changes in the refractive index are used to create superimposed transient population gratings and permanent structural gratings in Eu $^{3+}$ doped soda magnesium aluminosilicate (EDSMAS) glasses. The technique used to form the gratings is called four-wave mixing (FWM). Its nature is in nonlinear mixing of two laser "write" beams and laser "probe" beam to produce a fourth "signal" beam. This effect can be treated theoretically as a third order nonlinear process or, alternatively as Bragg scattering from a laser induced refractive index grating.

Many of the most interesting nonlinear properties leading to FWM are associated with impurities in the glass. Thus, the characteristics of the FWM signal can be altered by changing the defect distribution by means of varying the composition as well as the content of glass.

The experimental setup involves crossing two laser beams in the sample to form a constructive interference pattern in the form of sine wave. The light intensity in the peak regions of the pattern modulates the complex refractive index of the material compared to its value in the valley regions of the pattern. This creates a laser induced refractive index pattern. A probe beam passing through the sample in the presence of a refractive index grating is diffracted by the grating. By measuring the properties of the diffracted signal beam, all of the information the physical properties of the grating can be determined.

Figure 1.1 shows the typical experimental setup involving the alignment of laser beams

used for degenerate FWM and the condition for Bragg diffraction.
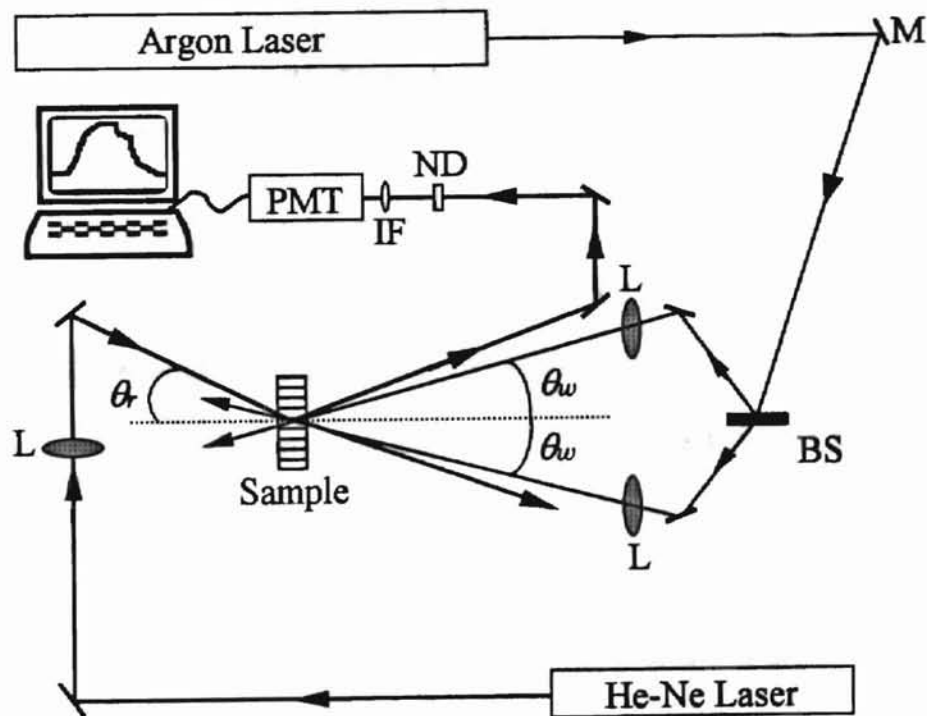
Fig.1.1. FWM experimental setup

The present research work is devoted to study the physical nature of holographic grating formation in Eu^{3+}-doped soda magnesium aluminosilicate (EDSMAS) glasses. Laser Raman spectroscopy will be employed in this work in an attempt to understand the mechanism underlying the holographic grating formation in these glasses. In particular, variation in the vibrational and structural properties due to the concentration changes of different individual components (Eu_2O_3, Al_2O_3 and Na_2O) in EDSMAS glasses will be studied.

Through the process of FWM experiment, Eu^{3+} ions of EDSMAS glass are excited by the laser write beam to the off - resonance $^5D_2$ – energy level. Radiationless relaxation from this excited state to the $^5D_0$ metastable level creates several high energy vibrational excitations (phonons) on the order of 1000 cm^{-1} (**Fig. 1.2**). This produces local structural change leaving the Eu^{3+} ions in a different configuration having a different index of refraction (R.C. Powell et al., 1987). In this sense, the role of high energy phonons ($\sim$ 1100 cm^{-1}) is believed to be crucial, since they fill the energy gap between the excited level and metastable $^5D_1$ as well as $^5D_0$ levels and provide the activation energy for some light modifiers to migrate in the glass network during FWM experiment. Thus, the permanent grating is formed due to the migration of light modifiers like Na and Mg from the bright to the dark regions of the grating.

G.S. Dixon et al., (1997) attributed the kinetics of the persistent gratings in rare–earth doped silicate glasses by the long range diffusion of small modifiers mediated by the hot-phonon field resulting from non-radiative decay of the rare-earth sensitizers. They suggested that the photorefractive efficiencies of these glasses
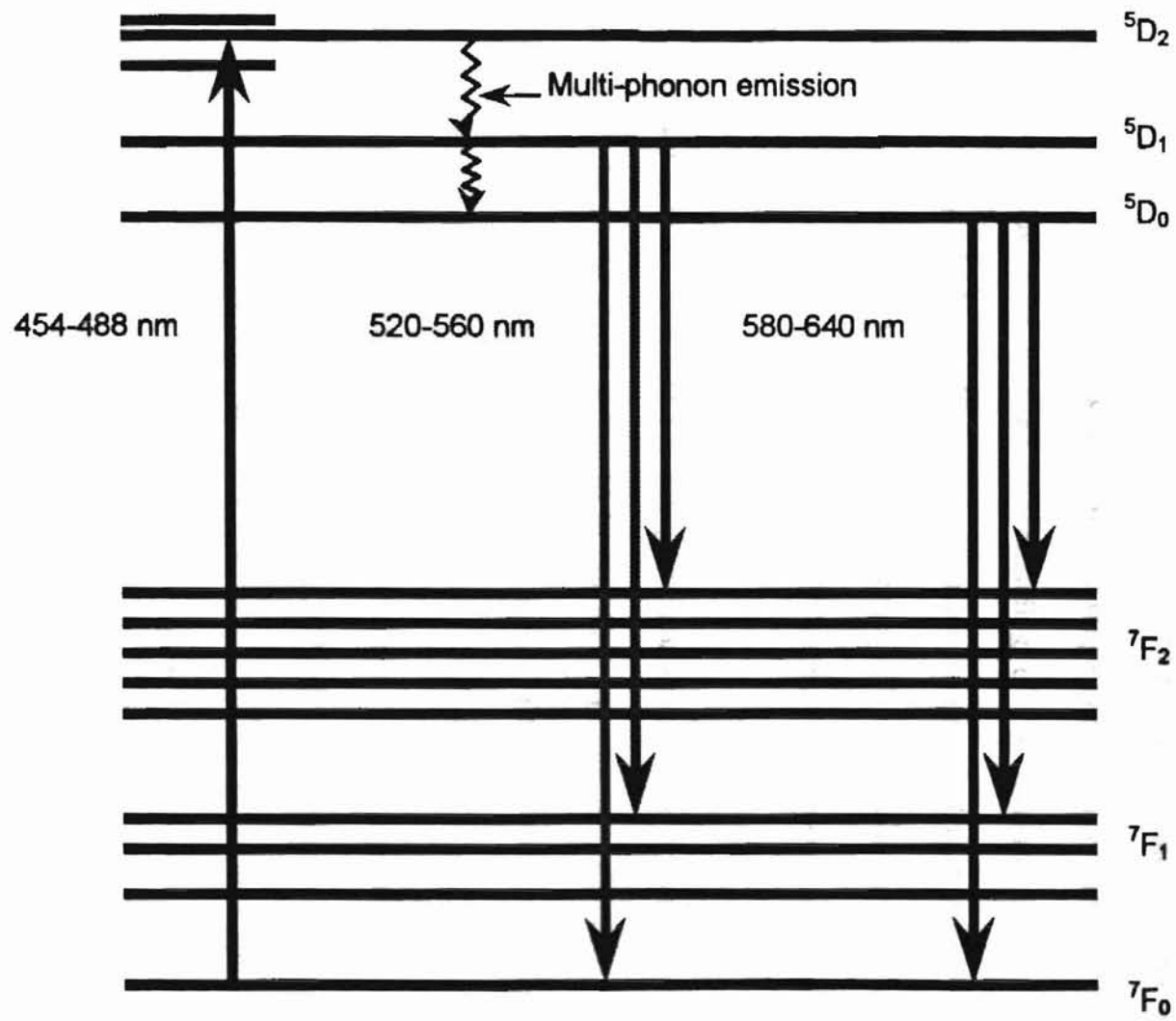
Fig.1.2. Eu^{3+} energy level diagram

might be improved through the increase of weakly bound modifiers or by the introduction of larger modifiers that tend to stretch the glass network.

We will use Raman spectroscopy to study the phonon vibrations in our glasses ranging from 50 cm^{-1} to 1300 cm^{-1}, This range includes the high-energy phonons, which are believed to be responsible for providing the channel for Na and Mg modifiers to migrate in the glass. This specific range of phonon frequencies (50 –1300 cm^{-1}) will give us more detailed understanding of the formation of holographic gratings in EDSMAS glasses. Thus, we will tailor the data on FWM strength signal in our glasses to their structural and vibrational changes by means of varying the content and the composition of the individual EDSMAS glass components using the Raman scattering data.

Recently it was found that the change in nonlinear index of refraction Δn (the signature of the FWM signal strength) in our glass samples was proportional to the number of the high energy phonons, the population of the excited Eu^{3+} ions and Al atoms present in the glass (Hamad *et al.*, 1998). The results of that work in the form of dependence of permanent change in the nonlinear index of refraction Δn versus different Eu_2O_3 and Al_2O_3 concentrations in EDSMAS glasses are presented on **Fig. 1.3** and **Fig. 1.4** respectively. We will discuss the results of Raman spectroscopic studies along with those of recent FWM experiments on our glasses and appropriate conclusions as well as suggestions for further research will be made.
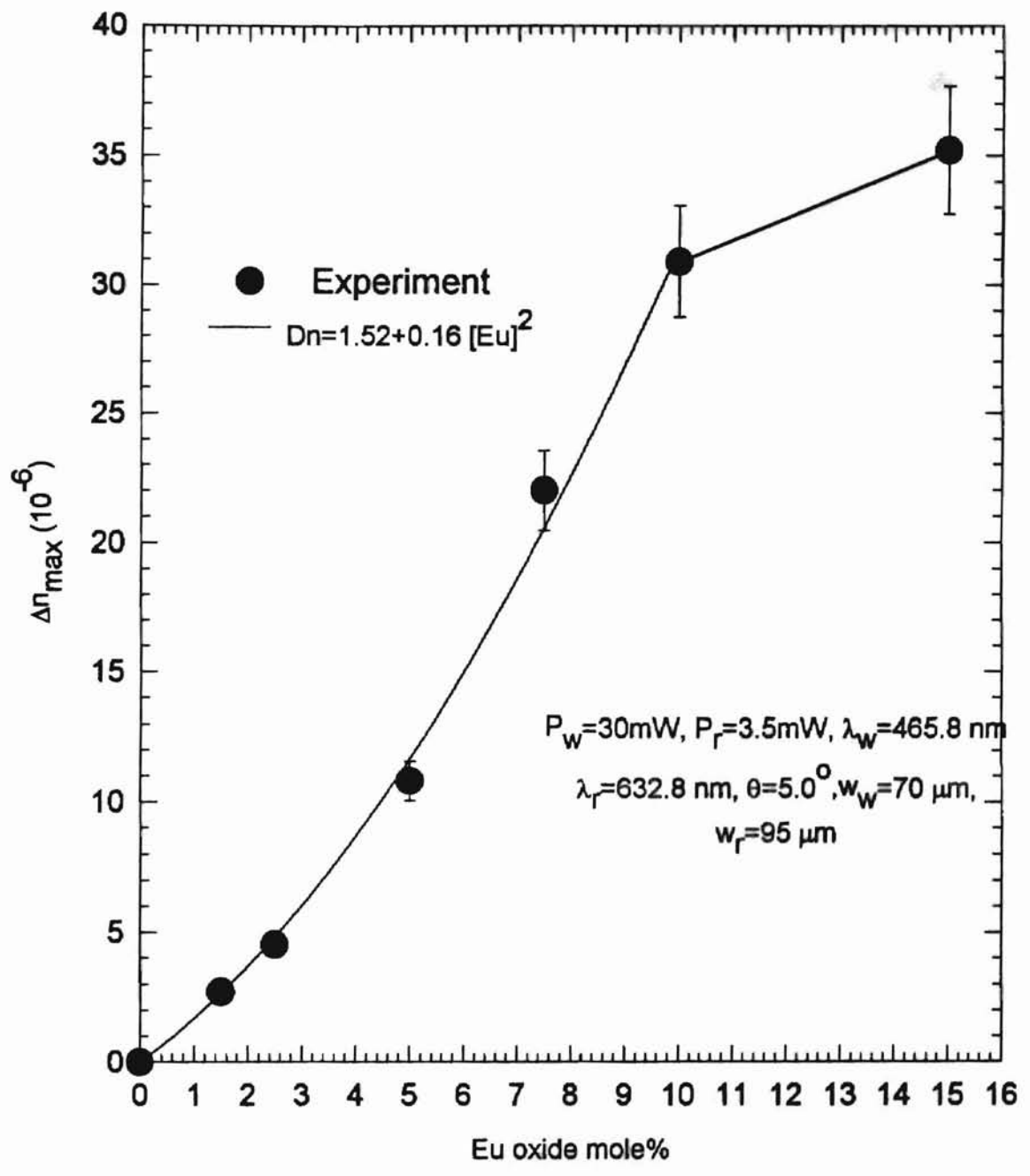
Fig.1.3. FWM strength signal vs. Eu oxide content in EDSMAS glasses
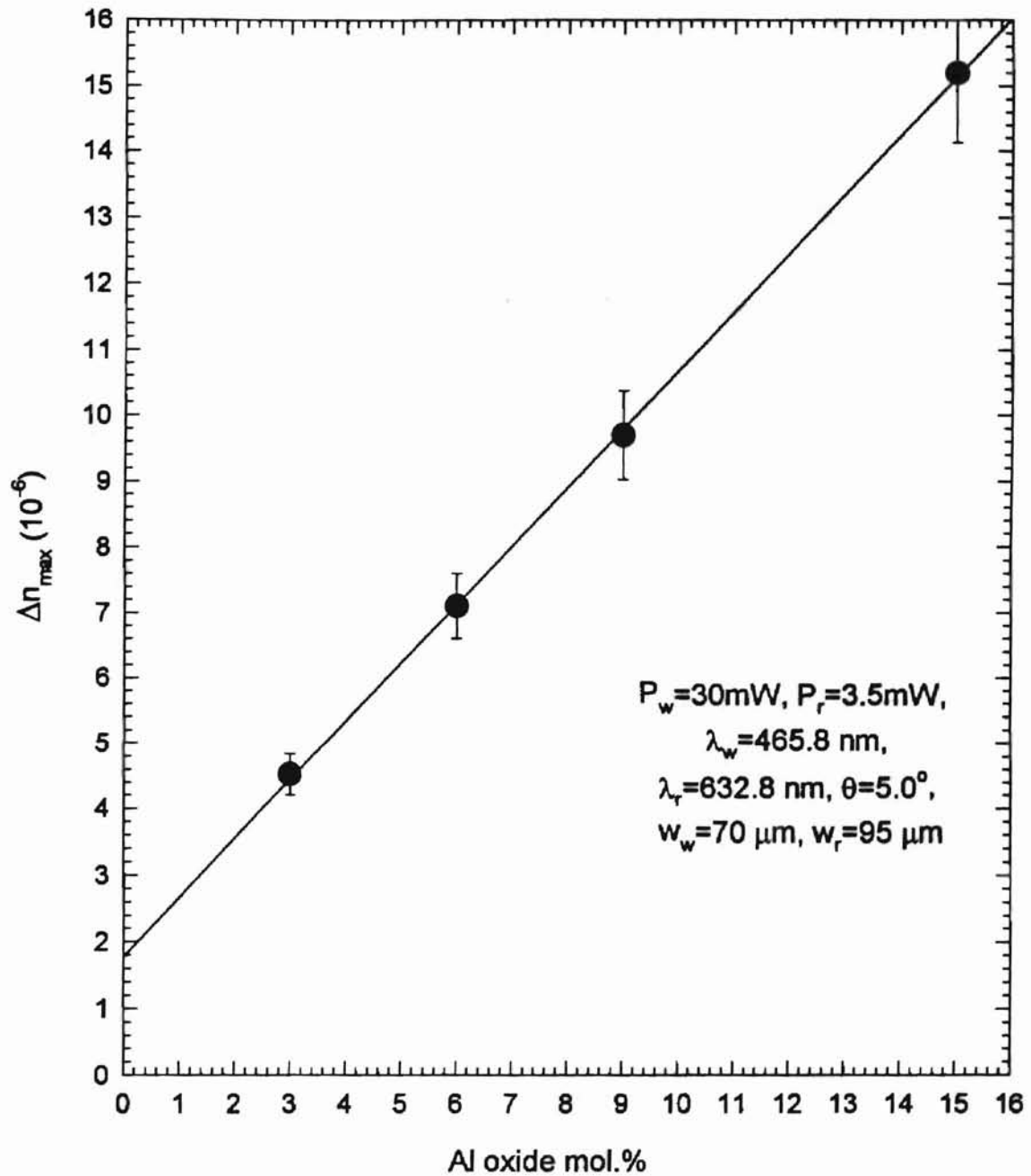
Fig.1.4. FWM strength signal vs. Al oxide content in EDSMAS glasses

CHAPTER II

THEORY

2.1.RAMAN SPECTROSCOPY IN GENERAL

The classical theory of the Raman effect has the following features. It is assumed that the electric field of the electromagnetic radiation incident on the material is an oscillating function:

$$E = E_0 \cos 2\nu\pi t \qquad (2.1.1)$$

The induced dipole moment caused by the external electric field in the first-order approximation is

$$\mu = \alpha E = \alpha E_0 \cos 2\nu\pi t \qquad (2.1.2)$$

For small displacements of the electron cloud a change in polarizability results:

$$\alpha = \alpha_0 + (\partial\alpha/\partial Q)* Q + ... \qquad (2.1.3)$$

Where Q is the normal coordinate. The harmonic approximation for the normal coordinate Q of oscillating atoms is:

$$Q = Q_0 \cos 2\nu_n\pi t \qquad (2.1.4)$$

The polarizability then becomes:

$$\alpha = \alpha_0 + (\partial\alpha/\partial Q)* Q + ... = \alpha_0 + (\partial\alpha/\partial Q) * Q_0 \cos 2\nu_n\pi t + ... \qquad (2.1.5)$$

Corresponding dipole moment is given by sum of three terms:

$$\mu = E_0 \cos2\nu\pi t \ (\alpha_0 + (\partial\alpha/\partial Q)* \ Q_0 \cos2\nu_n\pi t) = \alpha_0 \ E_0 \cos2\nu\pi$$

$$+ (\partial\alpha/\partial Q) \ (Q_0 \ E_0 \ / \ 2) \cos2\pi \ (\nu - \nu_n) + (\partial\alpha/\partial Q) \ (Q_0 \ E_0 \ / \ 2) \cos2\pi \ (\nu + \nu_n) \quad (2.1.6)$$

Where the first, second and third terms are represented by Rayleigh, Stokes Raman and Anti-Stokes Raman scattering respectively. The Stokes component of the Raman scattering stands for the phonon creation, while the Anti-Stoke component stands for the phonon annihilation. In the present work, we will be interested mainly in the Stoke branch of optical vibrations in the EDSMAS glasses.

In the quantum mechanical approach the population of atoms in higher and lower states are not equal but obey the Boltsman statistics, such that anti-Stokes to Stokes Intensity Ratio is

$$I_a \ / \ I_s = [(\nu + \nu_n) \ / \ (\nu - \nu_n)]^4 \exp \ (-h\nu_n / \ kT) \quad (2.1.7)$$

Induced transition probability matrix P_{nm} between m_{th} and n_{th} levels is:

$$P_{nm} = \int \Psi_m \alpha \Psi_n dQ \quad (2.1.8)$$

Here n is the ground state and m the excited state. In general, Raman scattering intensity I_{nm} is given by

$$I_{nm} = c(\nu_0 + \nu_{nm})^4 \ P_{nm}^2 \quad (2.1.9)$$

The intensity of the scattered light is dependent on the polarization character of the incident and scattered light and the symmetry of the polarization tensor α_{ij}. The polarization character is represented by a depolarization coefficient:

$$\rho(\theta) = I_{\shortparallel}(\theta) / \ I\perp(\theta) \quad (2.1.10)$$

Particularly, for amorphous (glassy) materials the Stokes Raman scattering intensity is (Galeener et $al.$, 1978):

$$I(\omega,\omega_0) = (h\upsilon E_0^2/4\pi^2 c^3)\{(\omega_0+\omega)^4 * \{n(\omega,T)+1\}/\omega\} * \sum C_b(\omega,\omega_0)\, g_b(\omega) \qquad (2.1.10)$$

Where b refers to the different bands, E_0 and ω_0 are the incident electric field and frequency, respectively, ω is the frequency of the Raman shift $c(\omega)$ is the coupling coefficient between the incident light and the modes of vibration in the medium, $g_b(\omega)$ is vibrational density of states for band b, $n(\omega,T)=1/[\exp(h\omega/kT)-1]$ is Bose –Einstein phonon distribution and $C_b(\omega,\omega_0) = \left| \sum_l P^l u_l^b(\omega) \right|^2$ is the coupling coefficient for the band b. Here P^l is the electronic polarizability and u^l is the normal displacement coordinate, where l refers to the 3N Cartesian coordinates of the atoms.

2.2. STRUCTURAL AND VIBRATIONAL PROPERTIES OF GLASS

It is well accepted that the short range order or the large range disorder are inherent for the glass structure which are characterized by three structural parameters: the bond length between the central atom and the nearest neighboring atom, the bond angle and the coordination number (Gan Fuxi, 1992). These three structural parameters for different glassy materials are also different from those of the crystalline state. In comparison with the crystalline state, the coordination numbers and the bond lengths are the same, whereas the bond angles have greater variation, which indicates that in the glassy state the presence of distorted tetrahedra takes place. For example, in most multicomponent silicate glasses the angle Si – O – Si bridges ranges from 120° to 180°, which provides freedom for the vertex angle

rotation and reflects the topological disorder of three dimensional structure in the glassy state.

It is very hard to represent various kinds of glasses with a unique structural model because each glass is different from others in structure and there is great variety of glass forming systems. According to Gan Fuxi (1992), the silicate glass systems are described as random polyhedra packing systems. The tetrahedra are connected at the vertex points and form three-dimensional structural networks. Some ions with greater radii, such as Al^{3+} can form tetrahedra and enter the network, or form octahedra outside the network; this is random network model, which can be regarded as the random packing of tetrahedra. The ions with even greater radii such as alkali metals and rare – earth ions locate at the vacancy of the polyhedron structure. In the study of variation rules of the dependence of optical and spectroscopic properties on the glass composition and structure, it is believed that the effect of coordination is the most important one. In other words, it is of the greatest significance to study in what kind of polyhedra the major ions are located.

As the atoms form lattices with definite symmetry in the crystal, the lattice vibrations can be treated with group theory. Glass has short-range order, so that its vibrational properties have their own features, however the remnants of translational symmetry always exist even in highly disordered solids, so some elements of crystal structure can also be observed in glasses with similar compositions. In particular, high wavenumber modes arising from short distance scale structures which appear as sharp bands in crystals, are broadened into density of states distributions in glasses and

often disappear completely in gels (White, 1990). Let us summarize some important features of the Raman spectra of glass.

1) The scattering light intensity of glass has nothing to do with the relative orientation of the incident light samples due to the fact that glass material can be treated with very good approximation as an isotropic medium, i.e. there are no specific directions in the glass material.

2) The unit cell number taking part in the vibration decreases obviously for some vibrational modes, which makes the Raman cross-section much smaller than that of the crystals.

3) Raman scattering peaks broaden due to the effect of disorder. The typical FWHM of the glass is on the order of $(50 - 150)$ cm^{-1} compared to $(5 - 10)$ cm^{-1} for the crystal. The increased bandwidths of the Raman lines of glass are taken to represent variations in the details of tetrahedral bond length and bond angle brought on by the disordered glass structure.

4) The coupling between the vibration and the light expressed as Raman scattering intensity which is realized by the relationship of induced polarizability, displacements of atoms and the number of atoms participating in the vibration per certain frequency.

5) The coherence length of the normal modes is much shorter than the wavelength (long wavelength approximation), leading to the ineffectiveness of the wave vector selection rules, and almost all normal modes appear in the light scattering event. Normal vibrations are classified into various bands, such as stretching bands, bending, rocking etc.

6) The vibrational frequency (phonon frequency) with the most neighboring atom is determined by the force constant K and the reduced mass M as $\omega^2 = K/M$. The relationship between the symmetrical (SS) and asymmetrical stretching (AS) vibrational frequency and the included angle Q of the bond can be shown (Gan Fuxi, 1982) as

$$\omega^2_{ss} = K\ (1+cosQ)/M$$

$$\omega^2_{as} = K\ (1-cosQ)/M$$

8) One of the main features of interest in the low frequency range is the Boson peak, identified with the existence of intermediate range order. This peak is due to the increase in the vibrational density of state caused by localized excitations (M. Lee *et al.*, 1999) which occurs typically in the range of 40 – 90 cm^{-1}. The band is seen to be asymmetric with a steep low wave number side and long tail on the high wave number side.

2.3. RAMAN SPECTRUM OF FUSED SILICA

The Raman spectrum of fused silica is very well known (**Fig. 2.3.1**). Three-dimensional representation of fused silica structure is shown on (**Fig. 2.3.2**). The interpretation of the vibrational properties of this material done by many authors [Matson W. (1983), Galeener (1982)] is as follows:

51 cm^{-1}: Boson peak
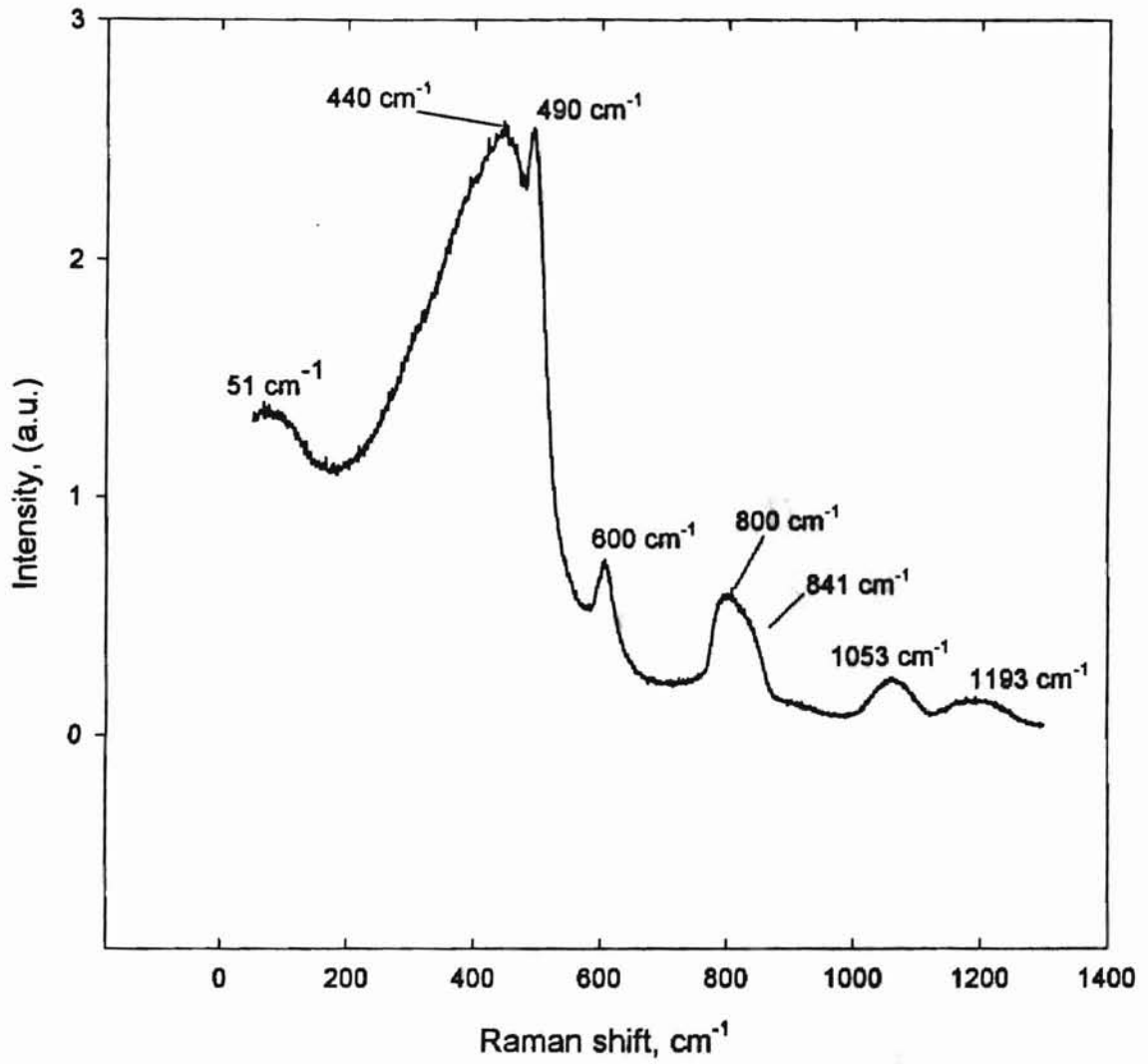
Fig. 2.3.1. Raman spectrum of fused silica
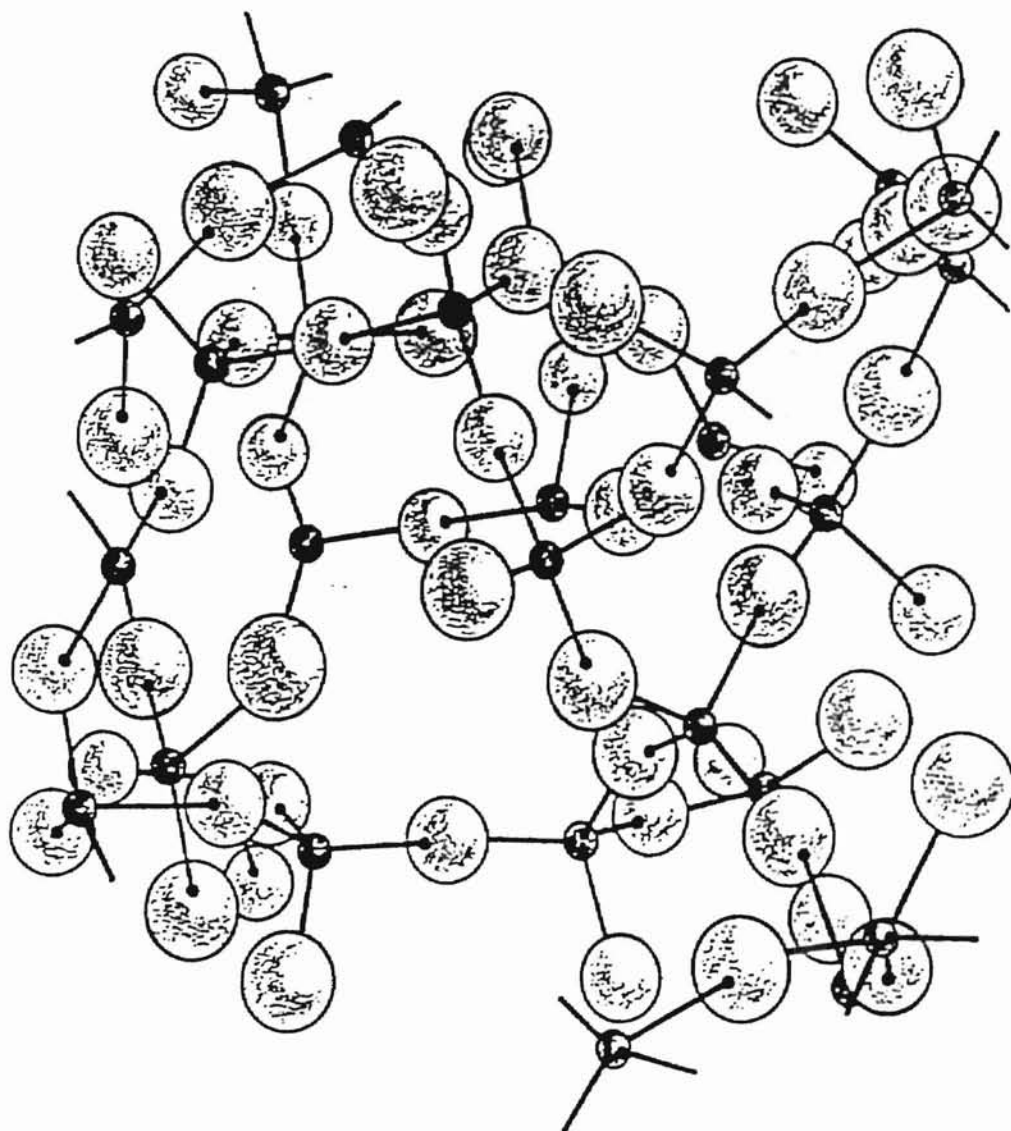
Fig. 2.3.2. Three-dimensional representation
of fused silica structure

440 cm^{-1}: Single dominant, asymmetric, rather broad and highly polarized Raman peak whose origin has been identified as due to symmetric stretching (SS) motion of the bridging oxygen atoms relative to the Si atoms in the three-dimensional network structure.

490 cm^{-1}: Sharp defect line, strongly polarized, with the narrow linewidth has been attributed to vibrationally isolated 4-membered rings of SiO$_4$ tetrahedra.

600 cm^{-1}: Defect line due to content of impurities such as Na up to 0.1% and F up to 0.3% or open Si-O-Si bridge as a result of glass manufacturing. Another explanation belongs to Gallener (1982), who proposed three - membered SiO$_4$ ring structures.

800 cm^{-1}: Transverse optical mode associated with the "bond-bending" type of motion in which the oxygens move approximately at right angles to the Si-Si lines in the Si-O-Si planes.

841 cm^{-1}: Longitudinal optical mode associated with the "bond-bending" motion in which the oxygens move approximately at right angles to the Si-Si lines in the Si-O-Si planes.

1053 cm^{-1}: Transverse optical mode associated with the "bond-stretching" vibration in which the bridging oxygens move in opposite directions to their Si neighbors, and roughly parallel to the Si-Si lines.

1193 cm^{-1}: Longitudinal optical mode associated with the "bond-stretching" vibration in which the bridging oxygens move in opposite directions to their Si neighbors, and roughly parallel to the Si-Si lines.

Bell et al (1970) showed that the spatial localization tends to be greatest at high frequencies and near band edges. If non-bridging oxygen atoms are present in the

structure, the frequency spectrum exhibits an additional band of very intense localization, associated with bond – stretching vibrations of non-bridging atoms. The measure of localization has been considered as the number of atoms effectively participating in a normal mode. In general, low frequency region of the Raman spectrum of the glass is characterized by the presence of relatively delocalized vibrations while the higher frequency range is characterized by the more localized phonons.

CHAPTER III

REVIEW OF THE LITERATURE

3.1. RAMAN SPECTROSCOPY OF MULTI - COMPONENT SILICATE GLASSES

3.1.1. RAMAN SPECTRUM OF BINARY Na_2O-SiO_2 GLASS

It is generally assumed that in silicate glasses the SiO_4 tetrahedra are connected at the vertices to form a glass network, while the various modifiers such as the alkalis and alkalines occupy interstitial sites in the network. Simple two-dimensional representation of sodium silicate glass is shown on (**fig. 3.1.1**). Some oxygens are bound to two silicons and are called bridging oxygen (BOs) atoms and some are linked to one silicon only and thus are called non-bridging oxygens (NBOs). In general, SiO_4 tetrahedral units containing one (two or three) bridging oxygens are called Q_1 (Q_2 or Q_3) species respectively. Nonbridging oxygens create coordination polyhedra for modifier ions. These features of the glass are explicit generalization of the structure of the crystalline silicates to the case of a disordered network, and are in agreement with x-ray diffraction results and Raman data. It is known that the chains or sheets are bound together by ionic NBO - alkali - NBO bonds.

Brawer *et al.*, (1975) showed that there is strong resemblance between glassy and crystalline spectra in the samples Na_2O - $xSiO_2$, $1 < x < 4$ which is consistent with a considerable amount of structural disorder of the glass. The most affected bands in
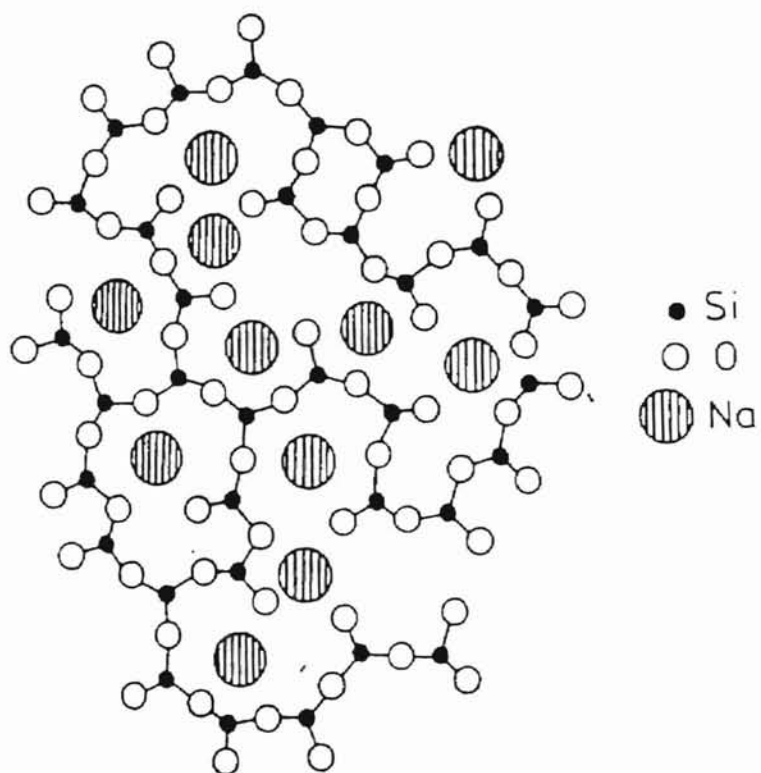
Fig. 3.1.1. Two-dimensional representation
of sodium silicate glass structure

binary alkali silicate glass are in the 900 cm^{-1} – 1200 cm^{-1} range of phonon frequencies compared to the spectrum of fused silica on the Fig. 2.3.1. This region of the spectra of the alkali-silicate glass is the result of highly localized Si-NBO stretching modes; relative intensities of these bands may be used to determine alkali distribution around SiO_4 tetrahedra. A completely random modifying cation distribution would lead to rapid destruction of the polymerized silica network with even small amounts of added cations because of the breaking of Si - O - Si bonds throughout the structure. DeJong et al (1981) presented the results of theoretical and experimental studies of silica - rich alkali silicate glasses, which indicated that Na cations have tendency to distribute themselves bimodally among local silicon environments. Metastable immiscibility in the high silica regions of Na_2O - SiO_2 glass systems (Charles, 1966 and Haller, 1974) has been taken to show that the cations distribution is non-uniform in the silicate systems.

Matson et al (1983) performed Raman vibrational study of the effect of different alkali ions with different content. In particular, due to the incorporation of 15 mole % of sodium in the network of vitreous silica they observed the following:

1) The bands at 440 cm^{-1} and at 800 cm^{-1} decrease in the relative intensity with increasing alkali content

2) The band first appearing at 490 cm^{-1} continuously shifts to higher frequency (500 cm^{-1}) with increasing alkali content but the frequency of the peak at 600 cm-1 is not affected much as far as the content of alkalis is concerned.

3) Intensities of sharp, polarized bands first appearing in the 500 cm^{-1} and 600 cm^{-1} regions of the glass spectrum increase rapidly with alkali content

4) The position of the 800 cm-1 band gradually shifts to lower frequency with increasing alkali content

5) A less intense, polarized band at 950 cm-1 appears with increasing alkali content. The sharp high frequency bands appearing near 950 cm^{-1} and 1100 cm^{-1} are the most dominant features in the alkali silicate glass spectra.

6) A sharp, polarized band whose intensity is alkali-content dependent emerges at 1100 cm^{-1} along with a high frequency polarized shoulder at ~ 1150 cm^{-1}. The shoulder appears to decrease in frequency and / or intensity with alkali content.

Matson et al (1983) interpreted Raman spectrum and assigned the bands as follows:

1150 cm^{-1}: Most probably this shoulder may be attributed to vibrations of NBO (i.e. Q'_3 species) that is structurally and vibrationally distinct from the Q_3 species producing the 1100 cm^{-1} band.

1100 cm^{-1}: Stretching of a single NBO on a SiO_4 tetrahedron (Si - O⁻) resulting from the presence of network modifying cations. A silicate sheet unit is capable of producing the band due to the combined vibrational contributions of each of the tetrahedral units containing one NBO. However, isolated Q_3 units formed by the introduction of alkali cations into a polymerized network must also contribute to the intensity of the 1100 cm^{-1} band.

950 cm^{-1}: results from Si - NBO stretching in SiO_4 tetrahedral units containing two NBOs (Q2 species). This vibrational mode is highly localized and the observation of this band cannot be used to infer the presence of extended sheet or chain structures.

600 cm^{-1}: more likely it originates from a localized vibrational mode. It may therefore originate from the same structure responsible for the 600 cm^{-1} SiO$_2$ glass band. This band may be characteristic of vibrationally isolated structures.

500 cm^{-1}: likely results from a highly delocalized vibrational mode of silicate network to which both bridging and nonbridging oxygen motion contributes. As such, its frequency is sensitive to alkali content and the degree of polymerization of the silicate structure.

440 cm^{-1}: is a characteristic of a fully polymerized 3D network and its presence in the high- silica alkali-silicate glass spectra indicates that regions of extended silica-like structure are retained in these glasses.

Matson *et al.*, (1983) concluded that smaller alkali species exhibit a greater tendency to cluster in pairs around SiO$_4$ tetrahedra (i.e. to form Q$_2$ species characterized by the 950 cm^{-1} band) than do the larger alkalis. The intensity at 1100 cm^{-1} is greater than at 950 cm^{-1}, indicating that Q$_3$ species are more abundant than the Q$_2$ species in all the silica-rich alkali-silicate glasses, irrespective of the type of alkali cations present. In addition to that it was shown that Q$_4$, Q$_3$ and Q$_2$ species are present in silica - rich alkali-silicate glasses, and that Q$_2$ species are relatively more abundant in glasses containing smaller alkali cations. However, Q$_3$ species appear in higher concentrations than Q$_2$ species in all glasses investigated. Thermodynamic properties of high-silica binary alkali-silicate systems have demonstrated that sodium ions tend to cluster into regions of relatively high alkali content. Sodium - silicate systems have metastable immiscibility regions that cause annealed glasses having compositions

within these regions to separate into two phases - one nearly pure SiO_2 and the other relatively high in alkali content.

3.1.2. RAMAN SPECTRUM OF TERNARY Na_2O - MgO - SiO_2 AND Na_2O - Al_2O_3 - SiO_2 GLASSES

Brawer et al (1976) showed that incorporating of magnesium ions into the network of binary sodium silicate glass leads to replacing of soda by magnesia. Alkaline atoms (e.g. Mg atoms) are the network modifiers. They enter to the glass network as doubly charged cations. The following long bridges are possible to create by introducing magnesium atoms: (-- Si – O – Mg – O – Si --). Thus, each alkaline ion is expected to create two NBOs.

The width of the band at 1100 cm^{-1} is increased due to increasing concentration of magnesium ions; thus, MgO creates disorder in the network of the binary silicate glass. In particular it was shown that MgO is much more effective in disordering the trisilicate than is CaO, as is clear from the considerable increase in the intensity of the 950 cm^{-1} peak relative to that of the 1100 cm^{-1} when MgO is added. From the Raman spectrum of $0.5Na_2O$ - $0.5MgO$ - $3SiO_2$ he suggested that the glass has large clusters or regions with very high SiO_2 content, which implies that alkali and alkaline atoms distribute themselves in the glass network non-homogeneously. Additional evidence for this is the strong peak at 450 cm^{-1} - a peak which is quite pronounced in the Raman spectrum of fused silica.

It is well known that the aluminum atoms are the glass formers rather than modifiers in the silicate glass. McKeown et al (1984) have indicated that sodium aluminosilicate glasses appear to become more polymerized with increasing the Al / Na - ratio. This suggests that Al stay in tetrahedral coordination throughout the glass series.

A vibrational mode in the far - infrared spectra of some sodium aluminosilicate glasses has been assigned by (Merzbacher and White, 1988) to the motion of network-modifying Na ions in large, interstitial sites. This assignment is confirmed by the direct relationship between Na content and peak intensity. In fully polymerized glasses along the SiO_2 - $NaAlO_4$ join, the number of network modifiers changes, but the environment surrounding each Na ions is the same. In simple Na_2O - SiO_2 glasses, depolymerization increases with added Na_2O, due to formation of NBOs, leading to gradual collapse of the tetrahedral structure around the Na ions and a rise in the vibrational energy.

Assuming that the oxygens form a rigid cage around the Na ions, the average force constant for the Na-O bonds ranges from 10 N/m in the fully polymerized glasses to 30 N/m in the most depolymerized sodium silicate glass.

The results of this study by far-infrared reflectance spectroscopy are in general agreement with conclusions based on MAS NMR and EXAFS analysis. These results are also consistent with the basic structural model in which Na acts as charge-compensating and/or network-modifying cations in glasses with Na/Al>1.

Mckewon et al.,(1984) assigned the bands in the Raman spectrum of silica - rich sodium aluminosilicate glasses as follows:

Low frequency band: broad, highly polarized due to acoustic modes involving Si cation motion and significant delocalization (i.e. small number of atoms). This band decreases in frequency while increasing in relative area with respect to increasing the ratio Al / Na.

485 cm^{-1}: It appears to be related to alumina content and has been previously interpreted to be due to a Si - O - Si vibrations (Macmillan, 1982). This band decreases in frequency while remaining roughly constant in relative area and width as the glasses increase in Al / Na - ratio.

595 cm^{-1}: This band might be assigned to a structural defect in the glass involving T-O NBOs vibrations (Sharma, 1979), the decrease in NBOs takes place as the Al / Na - ratio increases.(T represents former atom (Si or Al))

780 cm^{-1}: Si tetrahedral "cage" vibrations and Al tetrahedral vibrations. This band increases in the area and width with increasing Al / Na – ratio (Macmillan, 1982).

950cm^{-1}: Has been assigned to NBO content in glass structure. This band appears to decrease in frequency in the more Al-rich glasses.

1097 cm^{-1}: has been assigned to stretching of a single NBO on a SiO$_4$ tetrahedron (Si - O$^-$) resulting from the presence of network modifying cations.

3.1.3. THE EFFECT OF RARE EARTH IONS ON THE NETWORK OF BINARY, TERNARY AND QUATERNARY SILICATE GLASSES.

It is very well known that the rare earth ions incorporated into the silicate glass network are the dopants. Thus, their inclusion into the glass network leads to

proportional substitution of all glass formers and modifiers. Because the electrons at inner shell 4f of the rare-earth ions are shielded by the electrons out of 5s, p, d, so the effect of ligand field becomes weak. The energy levels of rare –earth ions in solids are similar to those of free ions. Raman spectra of the rare-earth silicate glass generally have many similar features for all off-resonance excitation wavelengths, though the spectrum itself can be noisy due to the absorption properties of the rare earth ions present in the glass. However, at the excitation wavelengths close to the resonance line the appearance of fluorescence bands as well as absorption contributions become inevitable. Therefore, the choice of the excitation wavelength is crucial in performing Raman scattering measurements on the rare earth doped silicate glasses.

There have been several investigations of structural changes in silicate glasses containing various rare earth ions with changes in glass composition using infrared and Raman spectra. Many studies have interpreted the vibrational spectra assuming the rare-earth ions behave as glass network modifiers rather than as network formers.

Krol D.M. *et al*, (1984) studied the Raman spectra of $20Na_2O - xR_2O_3 - (80-x)SiO_2$ glasses, where R = Sc, Y and La. The strongly polarized Raman band at 1080 cm^{-1} was assigned to the symmetric Si-O stretching mode involving a SiO^+ unit involving one NBO (Q_3 species), while the two less polarized Raman bands at 940 cm^{-1} and 1000 cm^{-1} were assigned symmetric and asymmetric Si-O stretching modes that are associated with SiO^+ units involving two NBOs (Q_2), respectively. They discriminated between the high frequency region (>500 cm-1) and the low frequency region (<500 cm-1). In the former, only vibrations involving network formers are

found; here we are mainly dealing with silicate networks. In the latter, vibrations of the modifier-oxygen bonds are found in addition to the network vibrations.

Kozuka *et al.*, (1987) measured and interpreted the Raman spectra for several compositional series in the $BaO - YO_{1.5} - SiO_2$ and $BaO - LaO_{1.5} - SiO_2$ glass systems. They used a deconvolution technique to identify various Raman bands. The deconvolution indicated Raman bands in the $(1050 - 1100)$ cm^{-1}, the 950 cm^{-1}, the 900 cm^{-1} and the 850 cm^{-1} regions, which were assigned to symmetric Si-O stretching motions in $(SiO_4)^{4-}$ units with one, two, three and four NBO's respectively.

Kohli *et al.*,(1993) performed a series of Raman measurements on rare-earth aluminosilicate glasses. Their spectra were simple and relatively free of sharp features. There was an indication that rare earth aluminosilicate glasses lack structure beyond the short range. The presence of a single broad band in the $(800 - 1200)$ cm^{-1} range suggested that a wide distribution of silicon-oxygen tetrahedra with different numbers of NBO and with different orientation with respect to each other could exist in their glasses. They showed that the incorporation of rare earth ions is expected to disrupt the connectivity of the network of tetrahedral groups, causing NBOs to form. The shift of this high-energy band to lower wavenumbers with increasing rare earth oxide concentration indicated that the average number NBO/tetrahedron increases with increasing rare-earth oxide content. The growth of more than one low wave number band in the Raman spectra of high samaria glasses may indicate that the presence of more than one coordination sphere for samarium ions in their glasses.

CHAPTER IV

DESCRIPTION OF EXPERIMENTS

4.1 RAMAN SCATTERING SETUP AND MEASUREMENTS

The Raman experimental setup utilized in this work is shown schematically in **Fig 4.1.1.** A Spectra Physics model 2020 Argon Ion Laser was used as an excitation source to produce monochromatic light. To get true Raman spectra with relatively low level of noise the wavelength of 457.9 nm was chosen so that the laser excited Eu^{3+} ions far from the resonance thus lowering the absorption and at the same time far from the fluorescence contribution. The laser output power was 300 mW. The emitted laser beam was directed into the bulk transparent sample of the parallelepiped shape placed on the horizontal holder. Right angle scattering configuration has been employed for obtaining polarized Raman spectra in our experiments. Scattered light was collected by a lens and passed through polarization analyzer and polarization scrambler into a Jobin-Yvon Ramanor U-1000 monochromator. Each monochromator features an asymmetric Czerny-Turner mounting with two symmetrical opening slits. The two diffraction gratings (1800 grooves/mm) rotate on a horizontal shaft parallel to the grating grooves. A concave lens of focal length 500 mm couples two monoctromators by imaging the exit slit of the first with the entrance slit of the second. Four mirrors, all with focal length 1m, divert the optical path. Light exiting the double monochromator was directed into an RCA C31034 Photomultiplier tube (PMT) cooled to $-20\,°C$ using a Products for Research
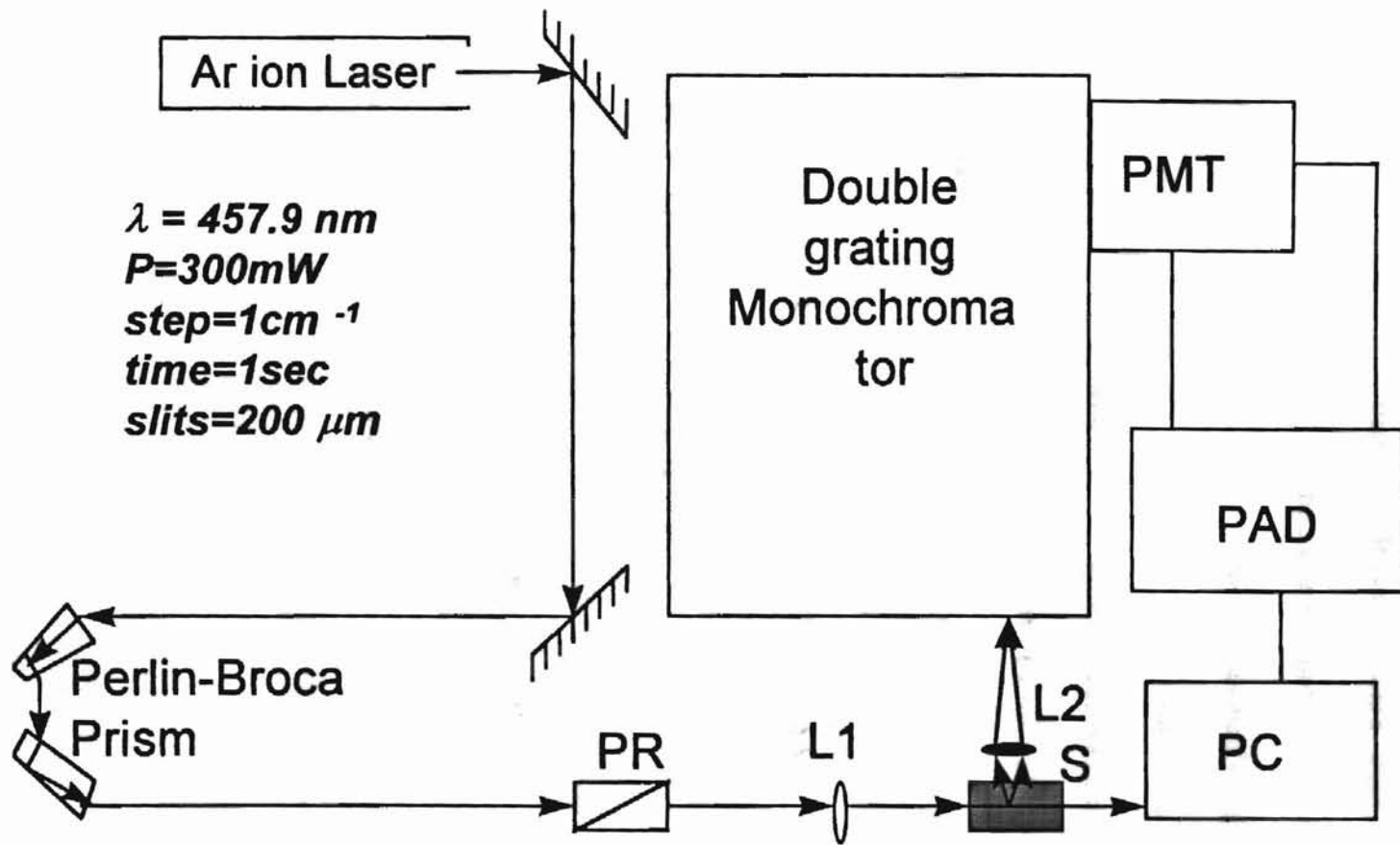
Fig.4.1.1. Experimental Raman scattering setup

thermoelectric cooling unit. The PMT coupled with a preamplifier and discriminator was connected to an IBM PC with Enhanced Prism software, used for scanning and data acquisition Scans are printed out using the same computer. All Raman scans were taken with an interval of 1 cm^{-1} every second to achieve reasonably high data resolution. The signal was maximized so that the peak signal-to-noise ratio was as high as 7:1 in the spectra to be presented. The optimal width of all four slits was chosen to be 200 microns. When the laser power was changed by +/100 mW, the overall structure didn't change. The Raman spectra of our glasses were very reproducible.

4.2. CURVE-FITTING ANALYSIS OF RAMAN SPECTRA

A number of studies have used deconvolution or curve-fitting techniques to separate unresolved bands into component sets (Furukava *et al*,. (1980), Mysen *et al*., (1982), McMillan *et al*., (1982), etc). When there are sufficient experimental data and individual band shapes are known, deconvolution methods allow a good solution for component band number, position and relative intensities within an unresolved envelope. The vibrational band shapes for glassy systems are not yet known. In most of the work on silicate glasses, the component Raman bands have been approximated by Gaussian functions. Although most of these studies give reasonable consistency with the observed spectra, none of the fits reproduces the experimental spectra exactly. This may be due to a variety of factors: noise in the experimental spectra, deviations of the true component bands from Gaussian shape, weak component bands not considered in the fit, errors in the chosen component band set, or baseline

corrections not accounted for. Such factors as the type of vibration, scattering geometry, optical properties of the detection system, and polarization of the bond contribute too.

For silicate glasses it appears reasonable to expect that the range of values of bond angles and bond distances are wider than in crystalline materials. Consequently, in glasses the half-width of a given band is greater than for the same band derived from a corresponding crystalline material.

In order to get as realistic fit as possible it is necessary to place some constraints on the fit procedure. In all fits, the major component bands must correspond to the unresolved peak maxima and slope changes in the experimental spectra. This constrains the minimum number of major components and their general position, and is more complete when carried out for both parallel (VV) and perpendicular (VH) polarized spectra. To summarize the results on the alkali and alkaline earth glass series, it is useful to consider their spectra in three regions: (1) the high frequency region between 1100 and 800 cm^{-1}; (2) the mid-frequency region between 800 and 700 cm^{-1} and (3) the low-frequency range between 400 and 700 cm^{-1}.

Mysen et al (1982) presented a peak fit technique to minimize the squares of the deviations between the observe and calculated Raman envelopes with Gaussian line shapes ($\chi^{2)}$. Thus, the attempt to decrease χ^2 – value and randomness of the residuals has been used to fit Raman spectra.

In present work, deconvolution peak fit technique has been utilized with the help of Peak Fit 4.0 Jandel Scietific Software to get detail information about the origin of the vibrations in the EDSMAS glasses. It should be noted that the instrumental

linewidth was not deconvolved from the Raman data. Gaussian peaks were used with no constraints. Overall background of the peaks has been taken as a linear. Crucial peak-fit quality characteristic is the coefficient of determination $r^2 = 1- SSE/SSM$, where SSE is the sum of squares due to error or sum of squared residuals given by:

$SSE = \Sigma\ \omega_i\ (y_{ei}-y_I)^2$

The y data value is y_I and the estimated y value is y_{ei}. The weight value is ω_i. The SSM, the sum of squares about the mean, defines a complete lack of fit, given by $SSM = \Sigma\ \omega_i\ (y_I - <y.>)^2$. The mean of the data values is $<y>$.

The maximum values of peak fit processing errors were found to be +/- 3 cm^{-1} in high frequency range, +/- 6cm^{-1} for mid-frequency range and +/- 8 cm^{-1} for low-frequency range. However, maximum deviation in the low-frequency broad continuum was observed to be equal 16 cm^{-1} which was due to highly unresolved structure within low frequency vibration spectrum of the glasses. From this data we see that the most accurate deconvolution result can be achieved only in the high frequency range. The overall result of peak fitting technique seams to be quite precise within gradual changes of positions and bandwidths of resolved bands as far as the content of glass modifiers and formers is concerned. Peak fit data were taken for all Raman scans and the detailed information on the structure including intensity, FWHM, peak area and peak position was obtained.

CHAPTER V

RESULTS AND DISCUSSION

5.1. THE EFFECT OF EUROPIUM CONCENTRATION ON THE NETWORK OF EDSMAS GLASS.

The Raman spectra of europium doped soda magnesium aluminosilicate glasses (EDSMAS) $[15Na_2O - 12MgO - 3Al_2O_3 - 70SiO_2]_{(100-x)}$ - $(Eu_2O_3)_x$ glasses with different Eu_2O_3 content (x = 0, 0.1, 0.5, 1, 2.5, 5, 7.5, 10, 15 mole %) have been taken (**Fig. 5.1.1**). All nine Raman spectra of this series were processed by the peak fit technique. An example of a typical peak-fit spectrum is represented for this glass with 2.5 mole % of Eu_2O_3 on **fig.5.1.2**. All spectra showed broad high frequency highly polarized bands in the (800 – 1200) cm^{-1} range associated with a wide distribution of different types of non-bridging oxygens existing for these glasses. This region of the Raman spectra in our EDSMAS glasses is expected to be due to wide distribution of silicon – oxygen tetrahedra with one, two and three BOs per tetrahedron, i.e. Q_1, Q_2 Q_3 species exist in our glasses (Fig. **5.1.3**). High frequency unresolved Raman band has been fitted by three peaks at about **1100 cm^{-1}**, **1015 cm^{-1}** and **965 cm^{-1}**.

A continuous shift of the high frequency **1100 cm^{-1}** peak from its initial position 1100 cm^{-1} to 1072 cm^{-1} has been observed (**fig. 5.1.4**) as we introduced Eu and
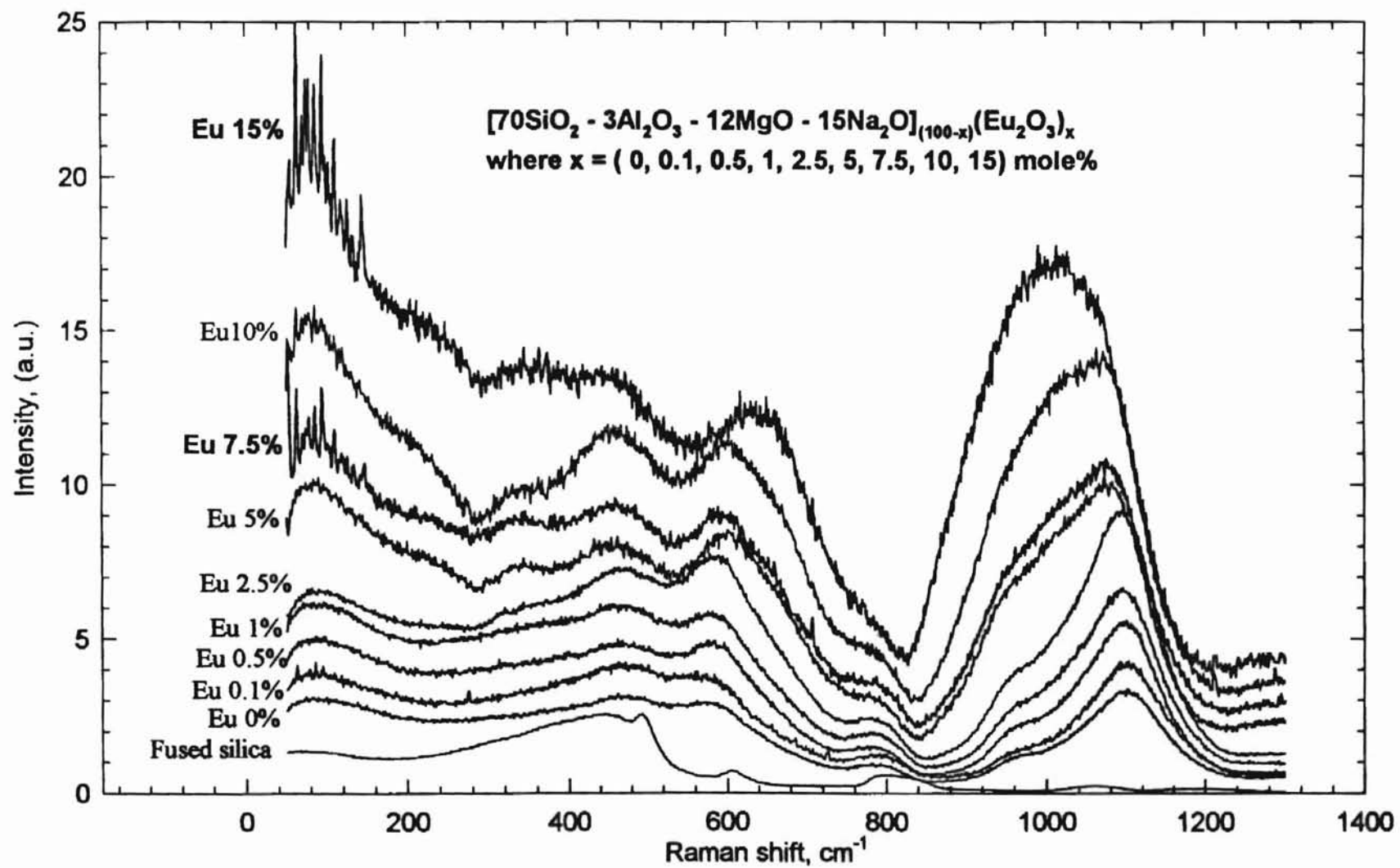
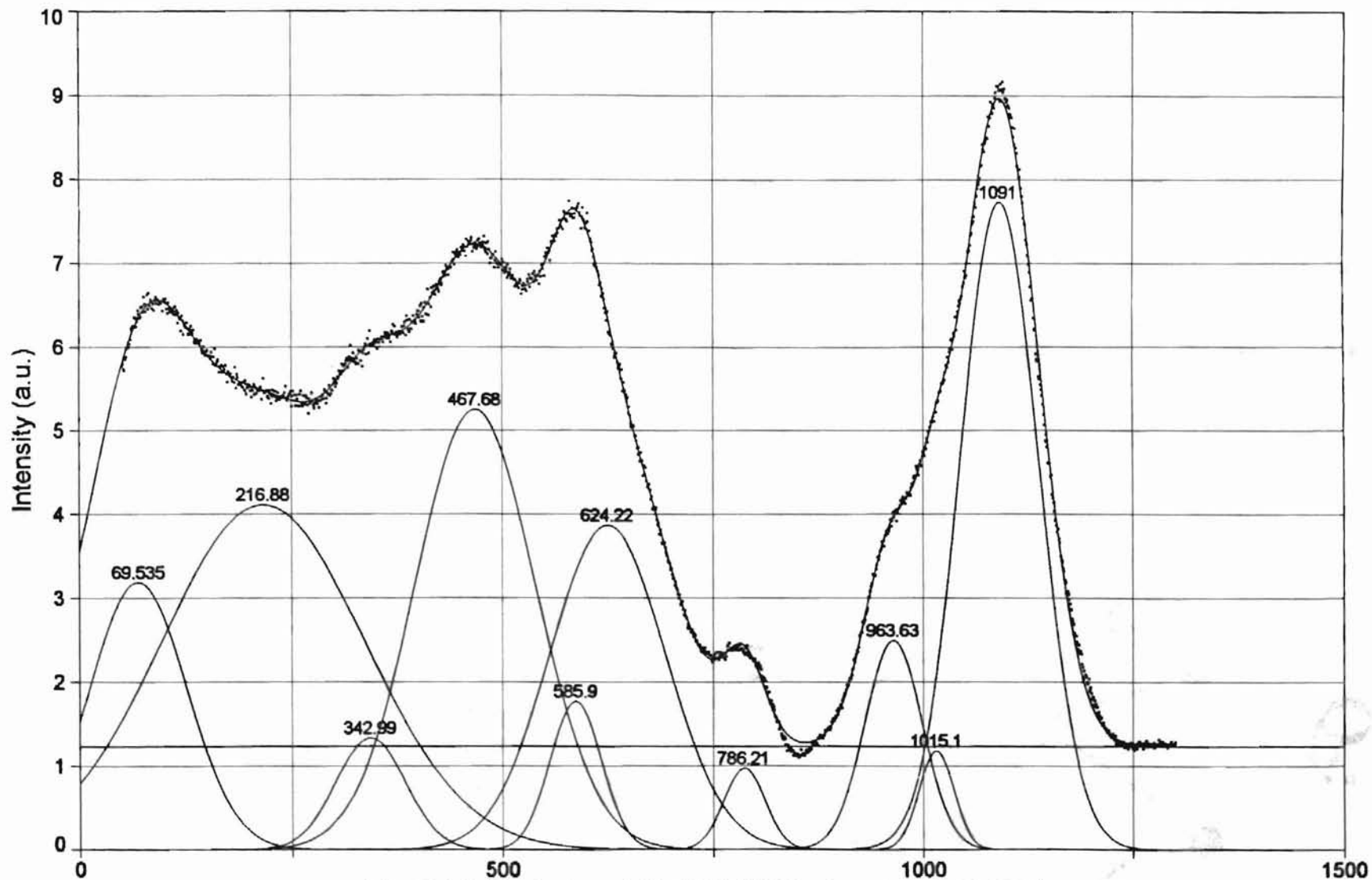Fig. 5.1.1. Raman spectra of EDSMAS glasses for different Eu oxide content

Fig. 5.1.2. Typical peak fit of EDSMAS glass (r^2=0.998955)

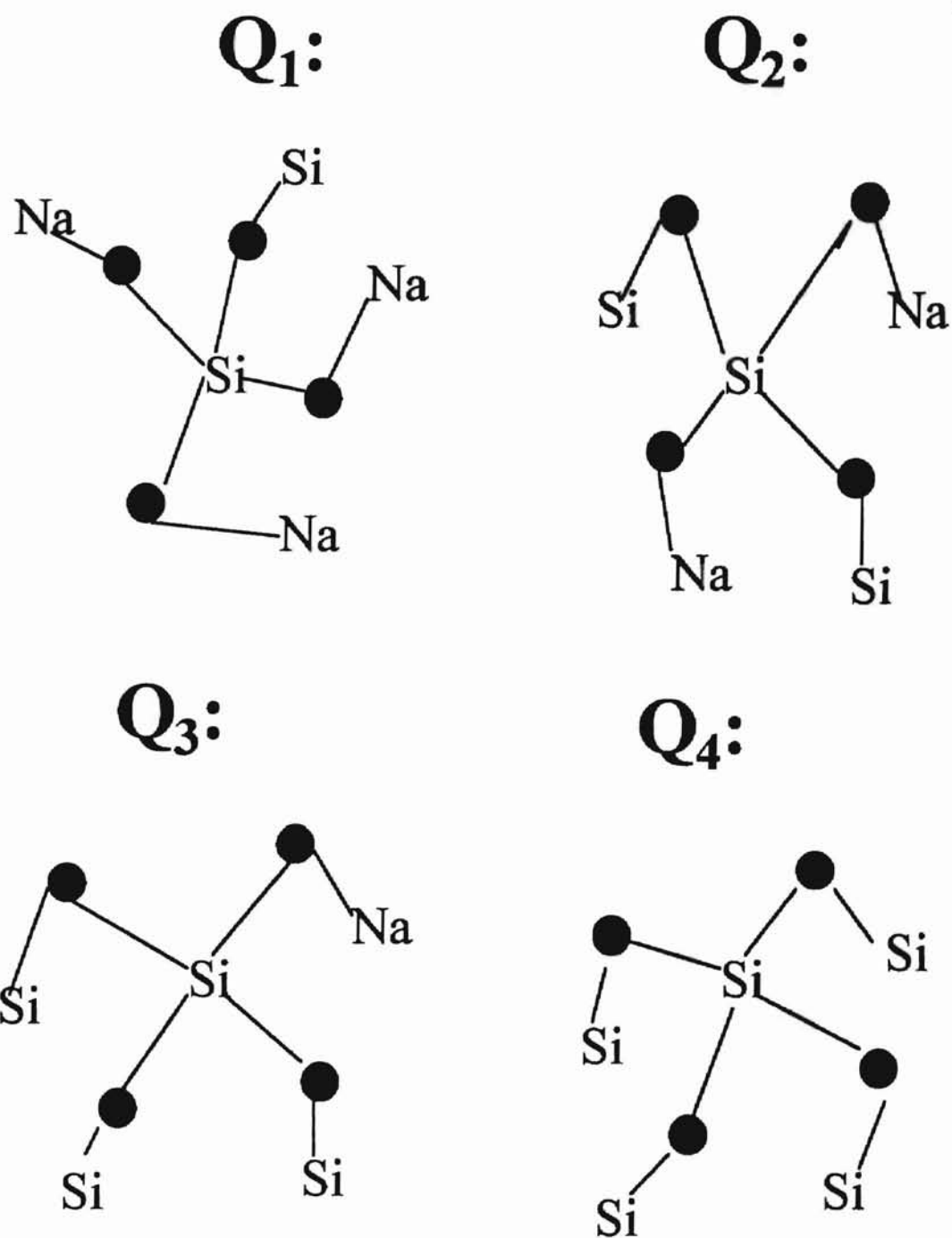**Q₁:**

Q₂:

Q₃:

Q₄:

Fig. 5.1.3. Q₁, Q₂, Q₃ and Q₄ species present in EDSMAS glass

increased its content up to 15 mole %. This strongly polarized Raman band is assigned mainly to the symmetric Si – NBO stretching mode associated with a SiO $^{4-}$ unit involving *one non-bridging oxygen (Q₃ species)* coordinated primarily with sodium and europium ions. The contribution of Si-BO stretching vibrations in this case is insignificant compared to the Si-NBO vibrations due to the presence of large number of NBOs in EDSMAS glasses. It is hard to resolve them in the high frequency range of multicomponent silicate glasses because the relative intensity of their band is very small in the fused silica Raman spectrum, (the latter doesn't contain NBOs, see high frequency range of the fused silica Raman spectra shown on fig. 2.3.1 and at the very bottom of fig 5.1.1). The downshift of 1100 cm^{-1} band was attributed to the fact that the average number of NBO per tetrahedra increased while increasing the rare-earth oxide concentration (Condrate, 1994). This effect takes place due to the formation of more NBOs by incorporating europium ions (modifiers) into the glass, the force constant of which is much less than that of bridging oxygens. In other words the bonding becomes more ionic rather than covalent. Krol (1984) suggested that a large electronegativity of the europium modifiers reduce the π-bonding of the Si – O$^-$ bond leading to a decrease to the bond strength and the force constant. The same considerations can be applied for **1015 cm^{-1}** and **965 cm^{-1}** bands. The width of the **1100 cm^{-1}** band has slightly decreased from 115 cm^{-1} to 103 cm^{-1} as more Eu is added, which could be accounted for by the decrease of disorder in the Q₃ species.

The frequency band at **1015 cm^{-1}** gradually shifts from its initial position 1015 cm^{-1} to 981 cm^{-1} as the europium atoms are introduced and their content is increased (fig. **5.1.4**). This effect takes place due to the same reason as in case of 1099 cm^{-1}
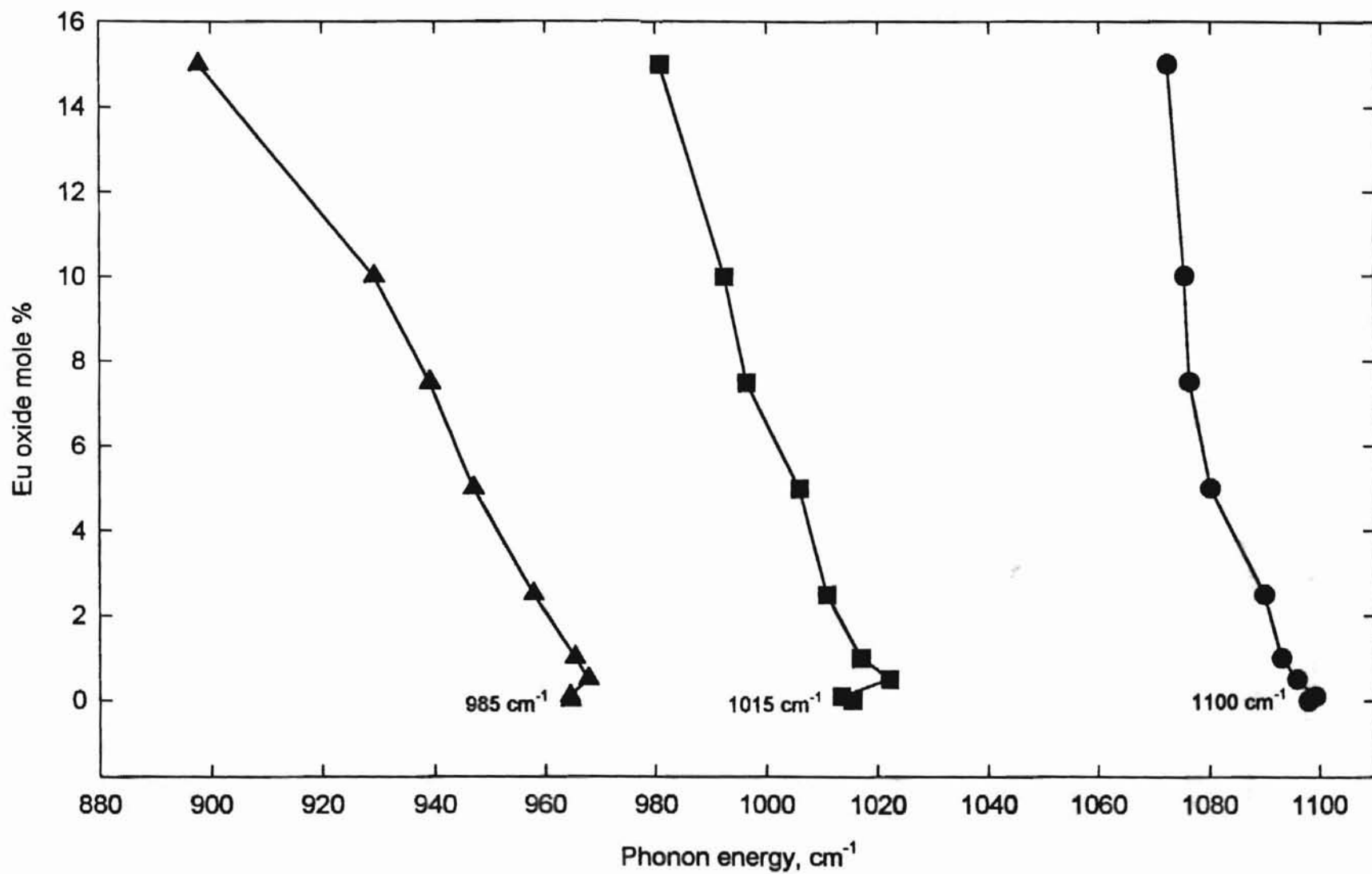
Fig. 5.1.4. High frequency band positions vs. Eu oxide content

band. This band was previously assigned to the Si – O stretching modes that are associated with SiO^{4-} involving *two nonbridging oxygens (Q_2 species)* coordinated primarily with europium. The width of this band gradually increased from 51 cm^{-1} to 124 cm^{-1} as more Eu was added.

The frequency band at **965 cm^{-1}** gradually shifts from its initial position 965 cm^{-1} to 899 cm^{-1} as the europium atoms are introduced and their content is increased (fig. **5.1.4**). This effect takes place due to the same reason as in case of 1100 cm^{-1}. It is reasonable to assign this band to the Si – O stretching modes that are associated with SiO^{4-} involving *three nonbridging oxygens (Q_1 species)* coordinated primarily with europium. The width of this band is gradually increased from 61 cm^{-1} to 80 cm^{-1} as more Eu is added.

From the deconvolution results of **fig. 5.1.2** we clearly see that the intensity of 1100 cm^{-1} band is significantly larger than that of 1015 cm^{-1} and 965 cm^{-1} bands, which suggests that the number of stretching Si-NBO vibrations associated with SiO^{4-} involving one NBO is much larger than that of involving two and three NBO. However, from the results of peak fit, the increase of europium atoms causes 1015 cm^{-1} and 965 cm^{-1} bands to grow relative to 1100 cm^{-1} band (fig. **5.1.5(a))**. Therefore, the number of symmetric Si – NBO stretching mode vibrations associated with silicate tetrahedra involving one non-bridging oxygen continuously decreases with respect to the number of stretching mode vibrations associated with those involving two and three NBOs as more europium atoms are added to the network of EDSMAS glass. Thus, the net effect of incorporating more europium ions is the growth of the NBO number. However, at high Eu concentrations (>7.5 mole %), 1015 cm^{-1} band
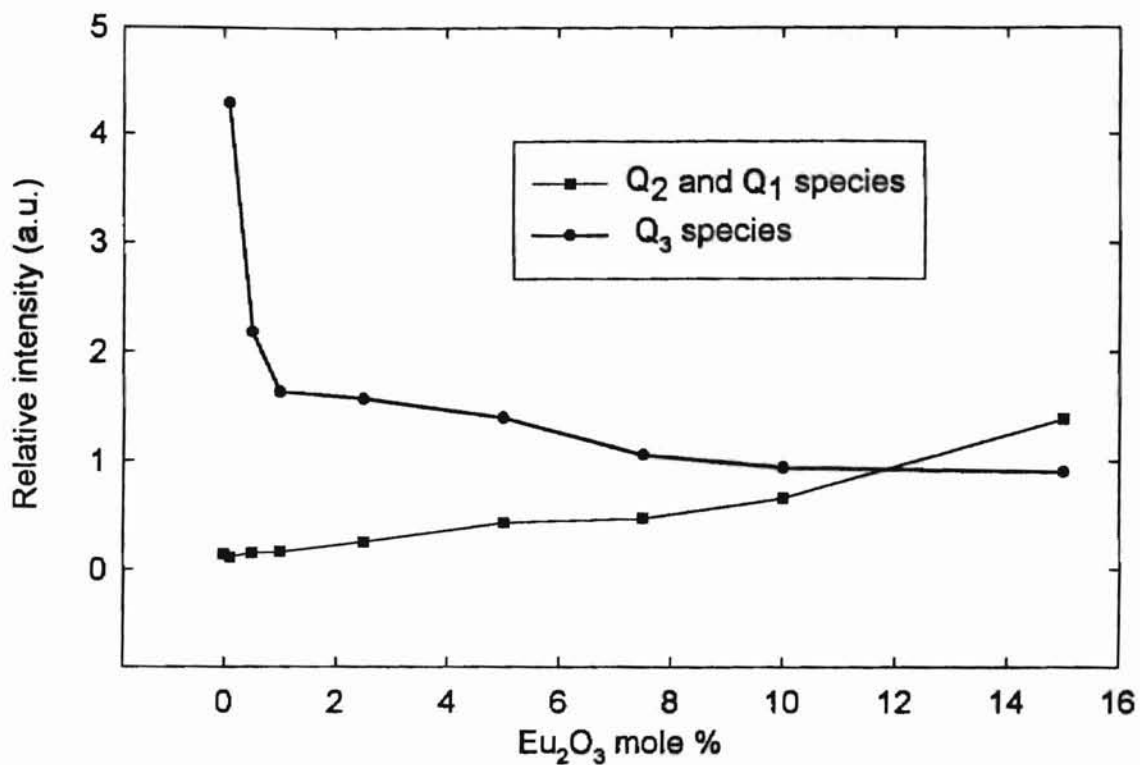
Fig. 5.1.5(a). The number of Q-species vs. Eu_2O_3 content
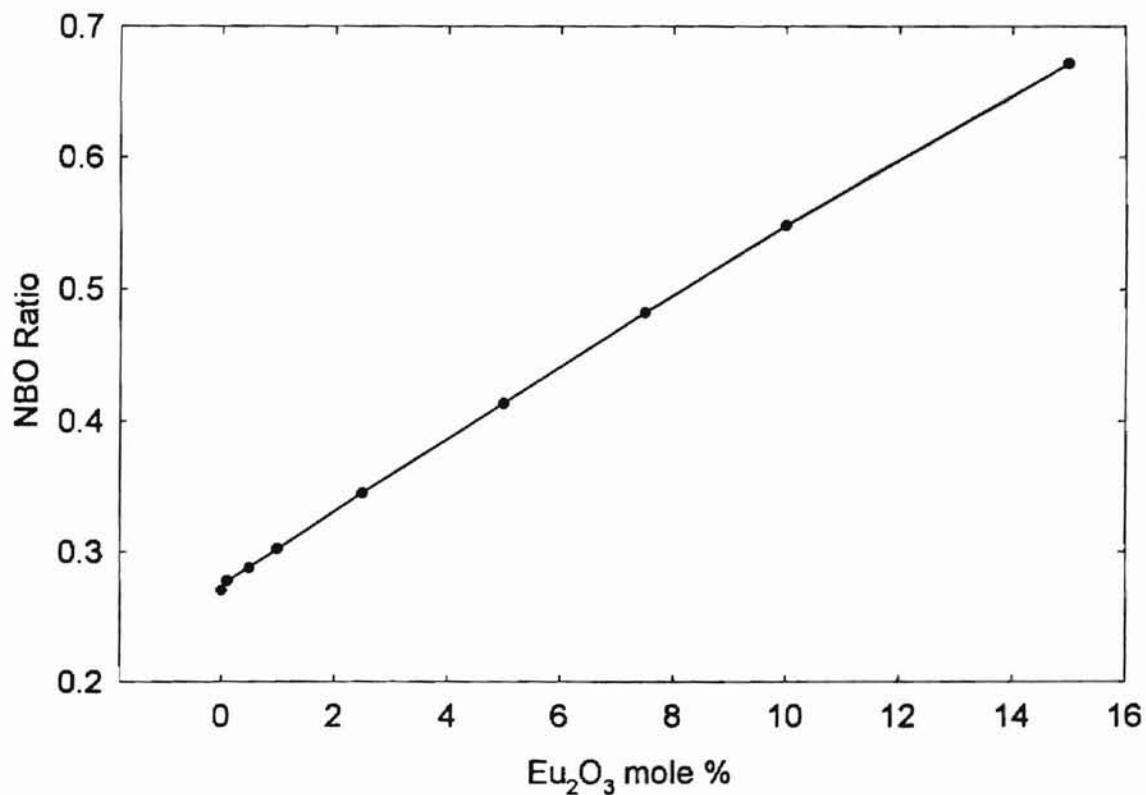

Fig. 5.1.5(b). Calculated NBO ratio vs. Eu_2O_3 content

increases more rapid than 965 cm^{-1} band suggesting that the whole glass network gradually is saturated by Q_2 species as the content of Eu ions increases. This effect is also supported by the calculation of the ratio of the number of NBOs to the total number of oxygens in these glasses (**fig. 5.1.5(b)**) for different content of Eu_2O_3 (0 – 15 mole %) based on the approach of A.Varshneya (1994). There is slight attenuation in the growth of the NBO ratio at high Eu concentrations according to this calculation.

From FWHM data of these three high – frequency peaks (see **Fig. 5.1.6**) as far as the content of europium is concerned, we can suggest that adding more europium atoms into the glass network leads to the formation of more disorder associated with a SiO^{4-} unit structure involving *two* non-bridging oxygens. In fact this disorder is more pronounced in those units where two rather than three Si – NBO stretching vibrations take place. This can take place because the bandwidth of 1015 cm^{-1} peak increases from 51 cm^{-1} to 124 cm^{-1}, but the bandwidth of 985 cm^{-1} peak broadens only from 61 cm^{-1} to 80 cm^{-1}. Thus, SiO^{4-} units having two NBOs are more disrupted by introducing Eu ions to the network rather than those having three NBOs. The disorder associated with a SiO^{4-} units involving one non-bridging oxygen has been slightly suppressed such that the bandwidth of 1100 cm^{-1} peak has been narrowed from 114 cm^{-1} to 103 cm^{-1} as more rare earth ions were added. Thus, the net effect of incorporating rare earth ions into the silicate glass network leads to formation of more disordered silicate glass network. This is possible since the Eu^{3+} ions entering the glass disrupt its overall connectivity.
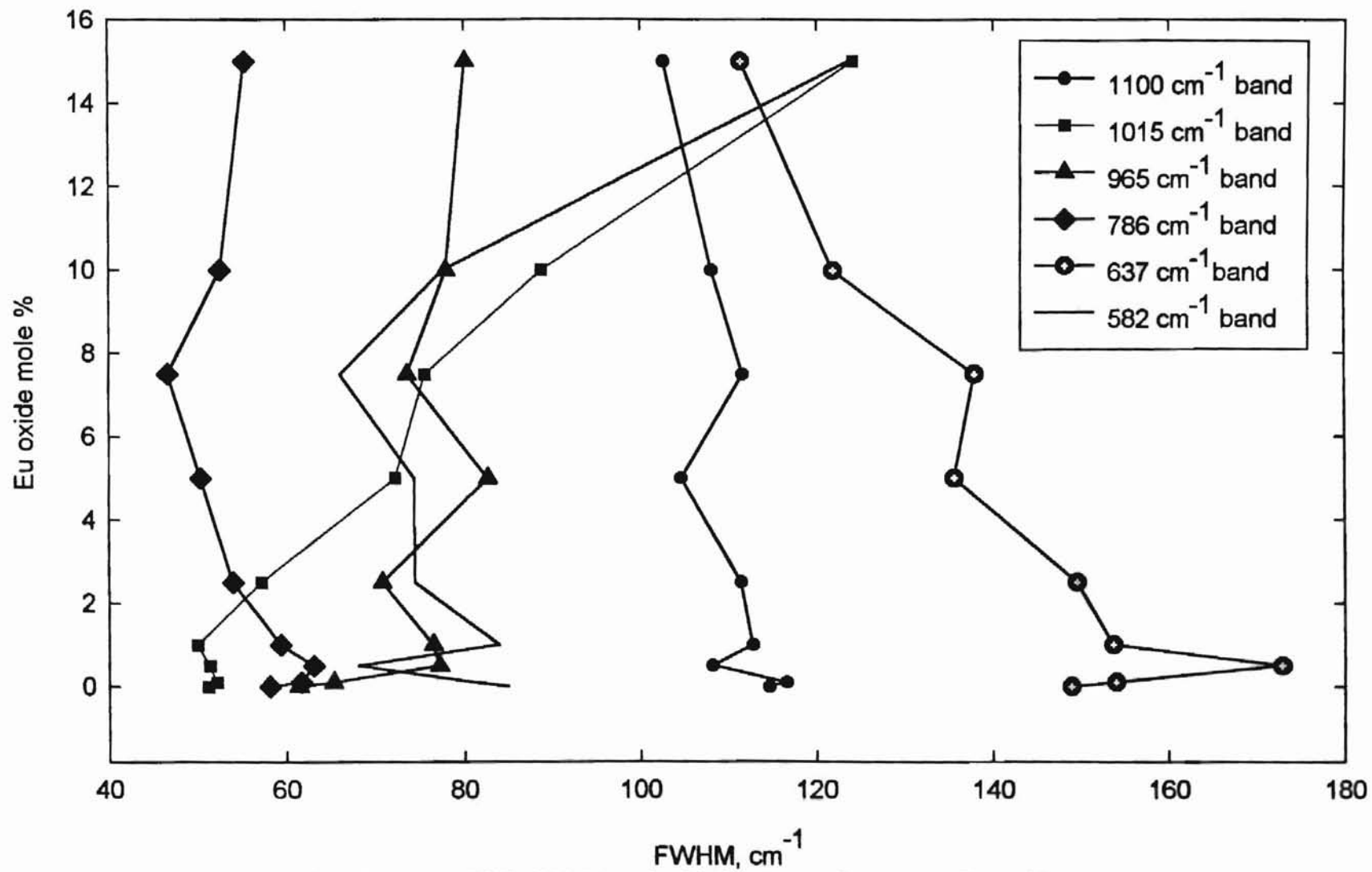
FWHM, cm^{-1}

Fig. 5.1.6. FWHM of high- and mid- frequency bands vs. Eu oxide content

The position of the peak at **786 cm^{-1}** continuously shifts toward the lower frequencies from 786 cm^{-1} to 770 cm^{-1} (see **Fig. 5.1.7**) by introducing Eu atoms and increasing their content up to 15 mole percentage. This peak was characterized by vibrations of silicon atoms in a tetrahedral "cage" of oxygens similar to vitreous silica earlier. In case of doping of europium atoms we decrease the content of silicon atoms, consequently, the vibration energy of silicon within a tetrahedral "cages" decreases. The bandwidth decreases from 58 cm^{-1} to 46 cm^{-1} once the Eu atoms are introduced and their content goes up to 7.5 mole %, however further increase of europiums up to 15 mole % leads to broadening of the bandwidth to 55 cm^{-1}. If these modes are associated mainly with motion of silicon against its oxygen "cage", it is possible that such vibrations will only be present for highly polymerized semi-rigid clusters.

The relative intensity of this band is the lowest among the other bands in Raman spectrum, which is most probably due to bending motion of silicon atoms within the oxygen cages rather than due to stretching motions. Its value decreases as the content of silica decreases. Thus, the decrease of the number of glass formers can be seen not only from the trend of band position but also from that of the relative intensity of the band.

The position of **637 cm^{-1}** asymmetric shoulder shifts toward the higher frequencies from 637 cm^{-1} to 682 cm^{-1} as the content of Eu$_2$O$_3$ increases up to 15 mole % (see **Fig. 5.1.7**). The FWHM of this peak decreases from 149 cm^{-1} to 111 cm^{-1} (see **Fig. 5.1.6**). The relative intensity of this band gradually decreases.

The position of the mid–frequency **582 cm^{-1}** band is changed from its initial position 582 cm^{-1} to 619 cm^{-1} as Eu is introduced and its content increases up to 15
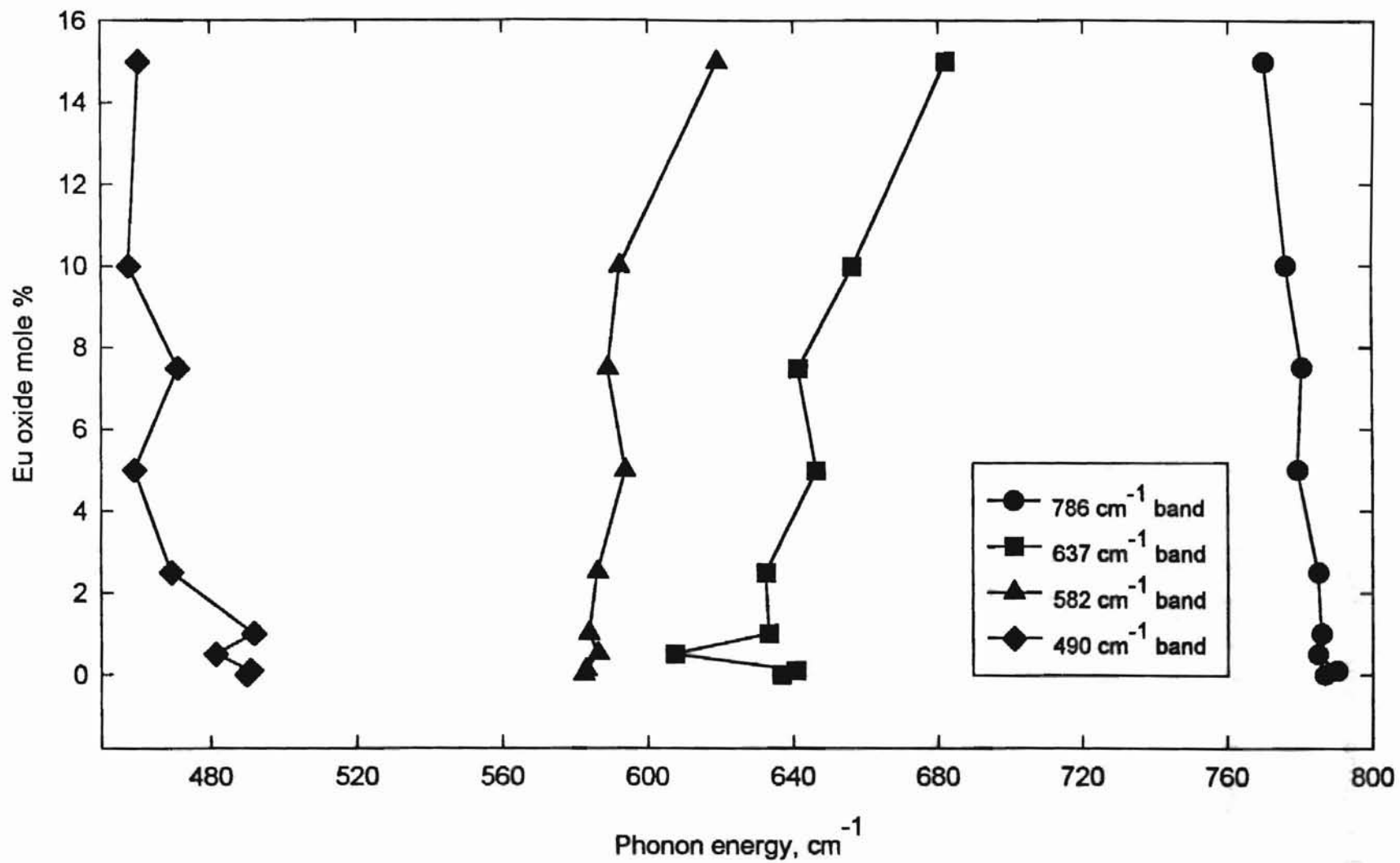
Fig. 5.1.7. Mid-frequency band positions vs. Eu oxide content

mole % (see **Fig. 5.1.7**). The FWHM is not affected by small content of Eu ions present in the glass (< 7.5 mole %); i.e. the effect of disorder does not take place for small rare earth ion concentrations. However, the glass structure becomes more disordered which is seen from the evidence that the width of the band increases from 77 cm^{-1} to 124 cm^{-1} when we further increase the content of Eu ions up to 15 mole % (see **Fig. 5.1.6**). This band decreases in the relative intensity while the content of Eu ions grows up to 7.5 mole %. We assigned this band to Si – O – Al bridge vibrations. Eu^{3+} ions in small concentrations cause these bridges to break and form non-bridging oxygens. The position of the small frequency band at **490 cm^{-1}** shifts toward the lower frequencies from 490 cm^{-1} to 461 cm^{-1} by increasing the europium ion content (Fig. **5.1.7**). This might be explained due to a substitution of host silicons and aluminums by the heavy Eu modifiers. However, at small concentrations of Eu atoms (< 2.5 %) the silicate glass network is not saturated yet by massive rare earth ions to make significant contribution to reducing the oscillator strength. The FWHM data indicates a general trend of increasing the width from 119 cm^{-1} to 204 cm^{-1} as the Eu atoms are introduced and their mole concentration is enhanced (see **Fig. 5.1.6**). This might be assigned to either Eu –O – Si or Eu –O – Al vibrations. It is known that the low-frequency modes are highly delocalized and it becomes reasonable to assume that the broadening mechanism of the 490 cm^{-1} band takes place after the incorporation of massive Eu ions leads to the formation of the regions with inhomogeneous distribution of disorder throughout the silicate tetrahedral structure. It is possible that the inhomogeneous distribution of disorder is due to the fact that fewer and fewer atoms per certain low frequency normal modes participate in the vibrations. The fact

that the structure becomes more disrupted due to the presence of rare earth atoms can also support the idea that Eu atoms enters the glass as network modifiers.

As the concentration of europium ions increases, broad bands become evident in the Raman spectra at the low frequency range, namely, appearance of a **new peaks** at **360 cm^{-1}** and **240 cm^{-1}**. These peaks become more pronounced at higher content of Eu$_2$O$_3$ (see **Fig. 5.1.1**). Substitution of the silicon atoms can take place and therefore the Eu-O vibrations or even inter-tetrahedral vibrations more likely characterize this band. Since Si-O and and Al-O bonds should be much stronger than Eu-O bonds and Si and Al atoms are lighter than Eu ions, modes involving Eu-O bonds should occur at lower wavenumbers than those involving Si-O or Al-O bonds. As a result, one is inclined to attribute the broad, low wave-number bands to europium – oxygen modes, which are not apparent in the spectra of EDSMAS glasses containing low concentrations of europiums. The formation of more than one band in this region for glasses containing high concentrations of europium may indicate that europium ions exist in more than one type of site or coordination sphere.

5.2. THE EFFECT OF ALUMINUM CONCENTRATION ON THE NETWORK OF EDSMAS GLASS.

Raman spectra of EDSMAS glasses have been taken with different concentrations (x = 0, 3, 6, 9, 15 mole %) of Al$_2$O$_3$ (Fig. 5.2.1). Aluminum oxide entered our glass at the expense of the reduction of the silica content. The
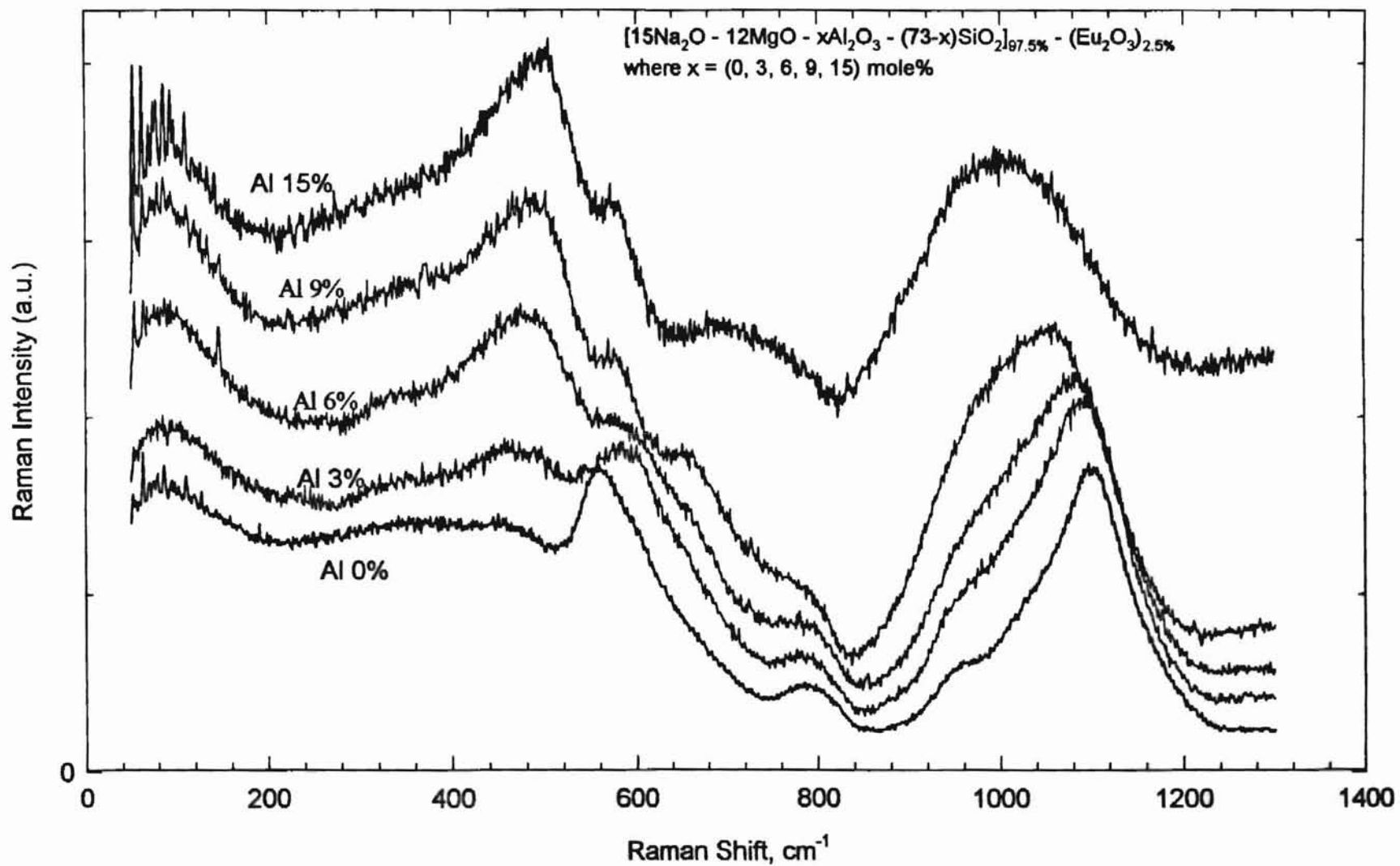
Fig. 5.2.1. Raman spectra of EDSMAS glasses for different Al content

deconvolution peak fit technique was similarly applied to get detailed information on the vibrational and structural properties of the glasses.

High frequency broad highly polarized band of the glass series in the (800 – 1200) cm^{-1} region of the Raman spectra indicated that a wide distribution of types of non-bridging oxygens exists for this series of glasses. This broad high frequency band has been peak fitted by three modes associated mainly with **1098 cm^{-1}, 1018 cm^{-1}** and **963 cm^{-1}** bands respectively. McMillan et al (1982) have attributed the Raman scattering in this region to vibrations with predominant silicon oxygen stretching character, with aluminum acting as perturbation on these vibrations. Thus, discrete frequencies were assigned to vibrations of the Si - (OAl)$_m$ (m = 1 - 4) units, with Si – O stretching frequency progressively decreasing upon increasing Al content. On the other hand, Mysen *et al.* (1981) have attributed the frequency downshift of the Si-O stretching vibration to the weakening of the Si-O bond in the Si – O – Al bridges and to the strong coupling of the Si – O and Al – O vibrations.

All three Gaussian bands shift their position toward lower frequencies as more Al atoms are incorporated into the glass network from 1098 cm^{-1} to 1039 cm^{-1}, from 1018 cm^{-1} to 957 cm^{-1} and from 963 cm^{-1} to 902 cm^{-1} respectively (**Fig. 5.2.2**).

A continuous shift of the high frequency **1098 cm^{-1}** peak from its initial position 1098 cm^{-1} to 1039 cm^{-1} has been observed as we introduce Al and increased its content up to 15 mole % (**Fig. 5.2.2**). This strongly polarized Raman band was assigned to the symmetric Si – NBO stretching modes associated with a SiO^{4-} units involving *one non-bridging oxygen*. Aluminum atoms entering the glass network are mostly tetrahedrally coordinated which give them glass-forming properties.
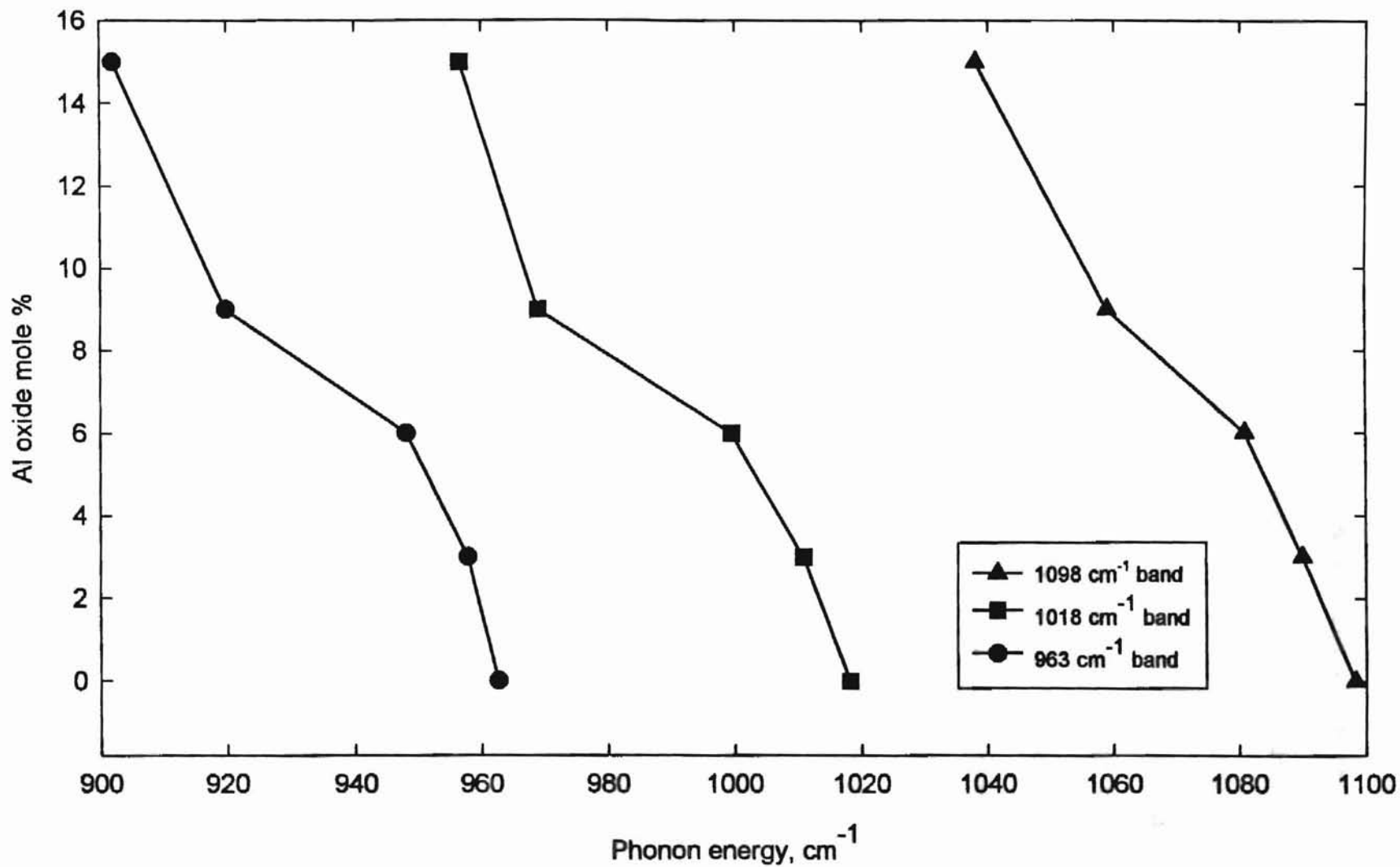
Fig. 5.2.2. High frequency band positions vs. Al oxide content

However, despite the closeness in mass of aluminum and silicon, their vibrational behavior might be quite different. Aluminum is a trivalent cation and therefore the electric charge-balance of tetrahedrally coordinated Al^{3+} must be maintained in order to accomplish an effective electric charge of 4+. The width of this band has been increased from 108 cm^{-1} to 145 cm^{-1} as more Al is added (see **Fig. 5.2.3**). This could be accounted for by the increase of disorder associated with Q_3 species. From the fact that the relative intensity of this band gradually goes down as the content of Al atoms increases we can infer that the number of NBOs associated with Q_3 species go down.

The frequency band at **1018 cm^{-1}** gradually shifts from its initial position 1018 cm^{-1} to 957 cm^{-1} as aluminum atoms are introduced and their content is increased (Fig. 5.2.2). This band was previously assigned to the Si – O stretching modes that are associated with SiO^{4-} involving *two nonbridging oxygens* coordinated by Eu atoms. The width of this band is gradually increased from 48 cm^{-1} to 97 cm^{-1} as more Al is added (Fig. 5.2.3). The relative intensity of this band was significantly changed with increase of Al content.

The frequency band at **963 cm^{-1}** gradually shifts from its initial position 963 cm^{-1} to 902 cm^{-1} as aluminum atoms are introduced and their content is increased (Fig. 5.2.2). This band was previously assigned to the symmetric Si – O stretching modes that are associated with SiO^{4-} involving *three nonbridging oxygens*. The width of this band is gradually decreased from 74 cm^{-1} to 59 cm^{-1} as the content of Al atoms increases up to 9 mole %, however further increasing the Al_2O_3 concentration up to 15 mole % leads to growing of the bandwidth from 59 cm^{-1} to 66 cm^{-1} (Fig. 5.2.3).
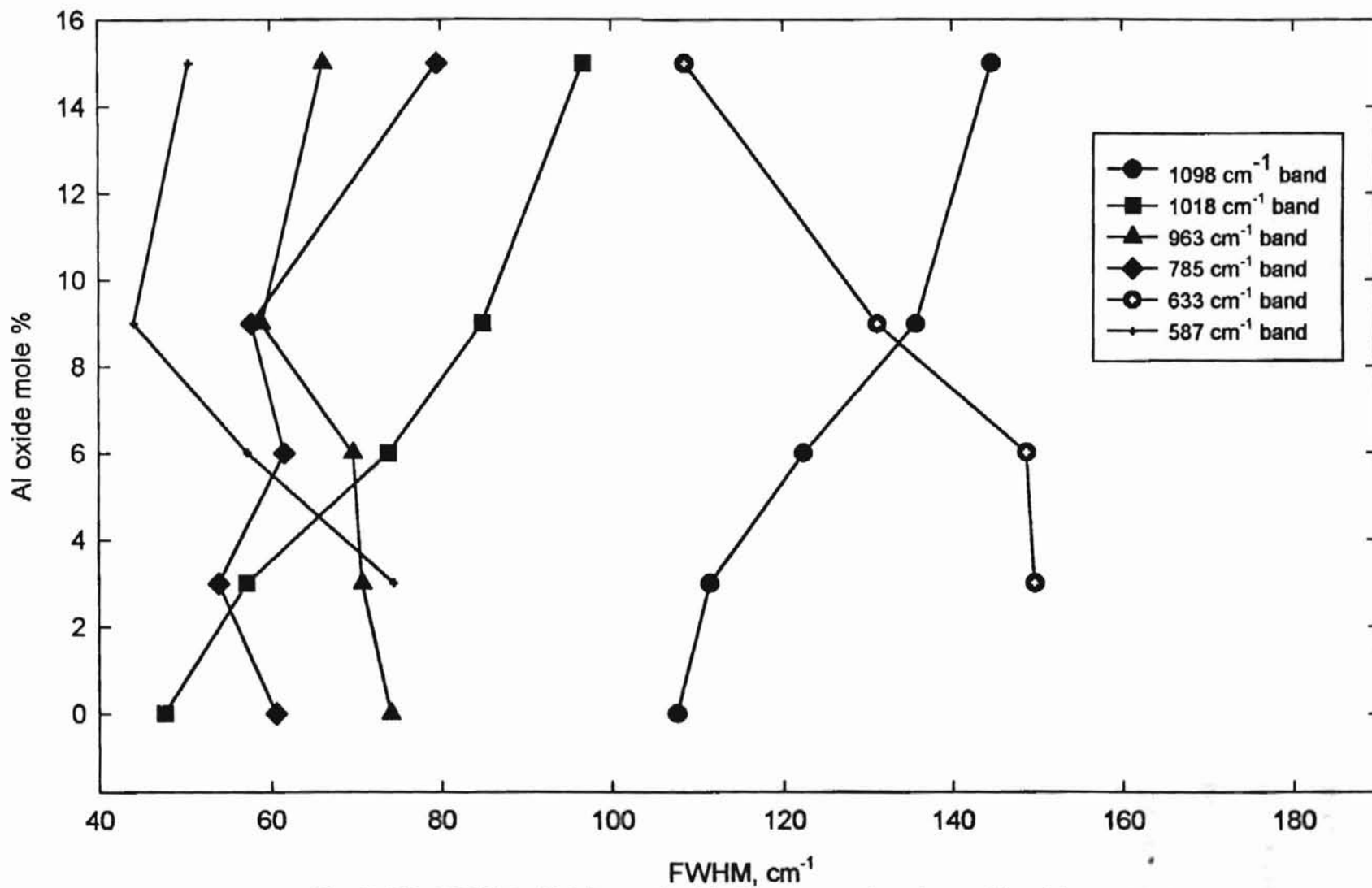
FWHM, cm^{-1}

Fig. 5.2.3. FWHM of high- and mid- frequency bands vs. Al oxide content

We plotted the relative dependence of Q_1 and Q_3 species versus the content of Al_2O_3 on the **Fig. 5.2.4 (a)**. The decrease of the number of non-bridging oxygens is clearly seen from this graph. This experimental results are also supported by the calculation of the ratio of NBOs to the total number of oxygens as a function of the aluminum content (Fig. **5.2.4 (b)**) made on the basis of the Varshneya's approach mentioned earlier in this dissertation.

The mid-frequency **785 cm^{-1}** peak suffers frequency downshift from its initial position 785 cm^{-1} to 725 cm^{-1} as the content of aluminum increases (**Fig. 5.2.5**). This band is characterized by the vibrations of Si and Al atoms on tetrahedral "cage" of oxygens. The vibrational energy of the Si – and Al- tetrahedral "cage" decreases because of aluminum substitution for silicon. If these modes are associated mainly with motion of silicon against its oxygen "cage", it is possible that such vibrations will only be present for highly polymerized, semi-rigid network. The bandwidth of this peak is not changed as we increase Al content up to 9 mole %. However, further increase of aluminum atoms up to 15 mole % causes the width to change from 58 cm^{-1} to 80 cm^{-1} (Fig. 5.2.3). This takes place most likely because the content of Al atoms in the host of the glass becomes equal to the number of Na atoms, i.e. the content of glass formers equals that of alkali modifiers in the glass host. The relative intensity of this band is the lowest among the other bands (replica of fused silica) in Raman spectrum and its value steeply decreases as the content of silica decreases. Thus, the number of tetrahedral "cage" vibrations goes down as the content of silicon glass formers decreases.
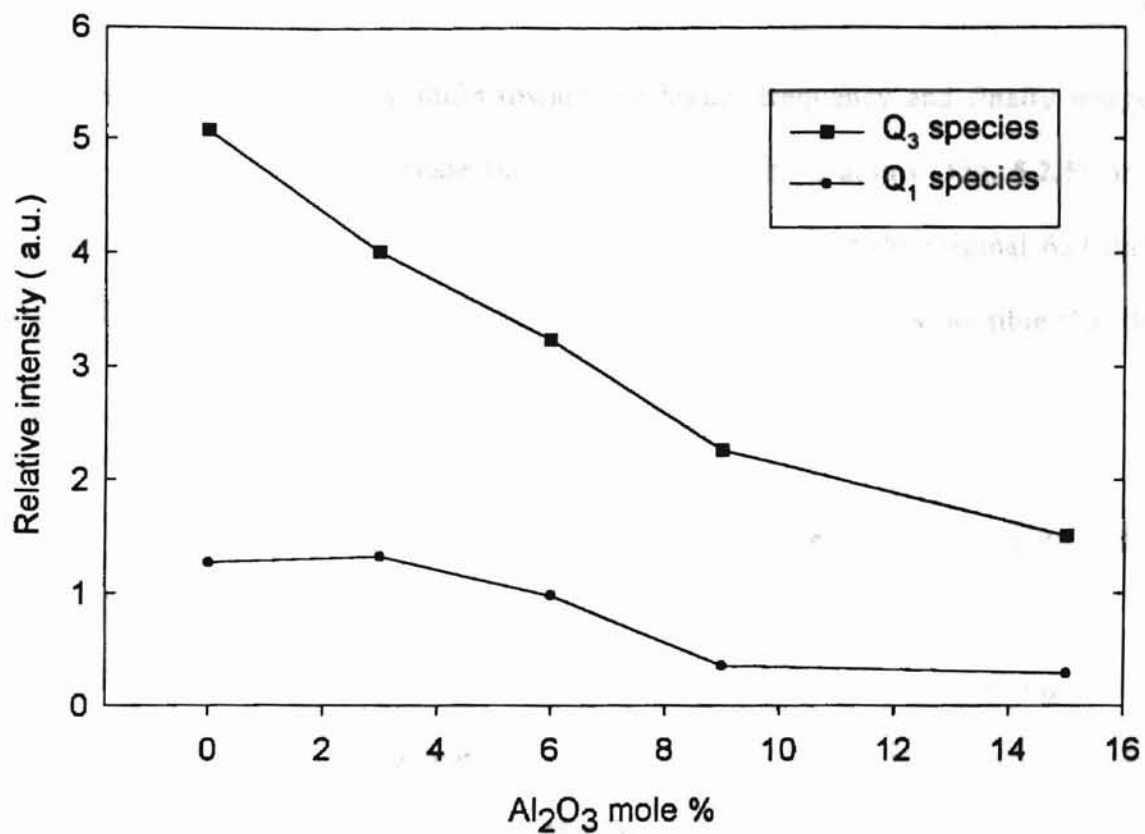
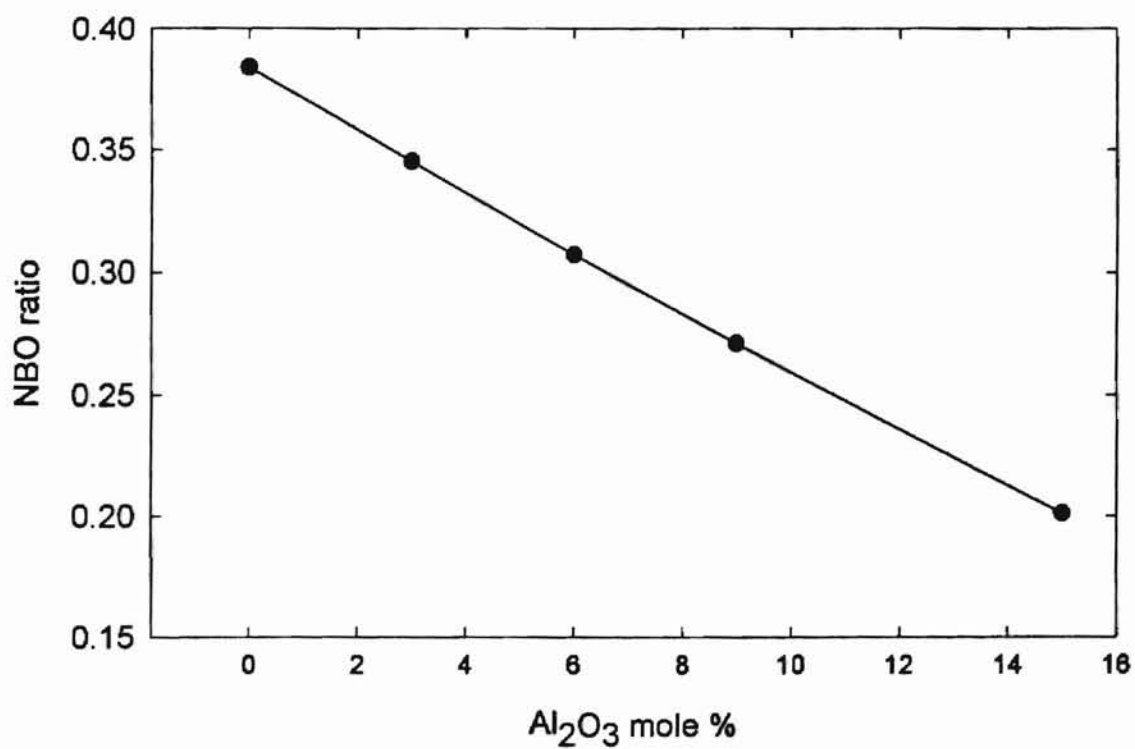Fig. 5.2.4(a). The number of Q - species vs. Al content

Fig. 5.2.4(b). Calculated NBO ratio vs. Al oxide content

The **633 cm**$^{-1}$ band gradually shifts toward the higher frequency and finally merges with 795 cm^{-1} band as we increase the content of aluminum atoms (**Fig. 5.2.5**). It is not clear whether new bands appear in the region 700 cm^{-1} or the original 633 cm^{-1} band suffers frequency up-shift at high concentration of Al_2O_3. It is possible that the new types of coordination spheres will form due to high content of Al_2O_3 present in EDSMAS glass.

The **587 cm**$^{-1}$ band slightly shifts toward the lower frequencies from its initial value 587 cm^{-1} to 581 cm^{-1} (**Fig. 5.2.5**) and its bandwidth has been narrowed from 74 cm^{-1} to 51 cm^{-1} (**Fig. 5.2.3**) and the relative intensity of this band did not change as Al oxide is introduced and its content increases up to 15 mole %. This band might be assigned to the vibrations of Si – O – Al bridges where Al atoms are tetrahedrally coordinated. Since with an increase of Al content, the content of silica decreases, then the average number of Si – O - Al bridge vibrations does not alter, therefore, the relative intensity of this band stays the same.

The **469 cm**$^{-1}$ peak changes its position from 469 cm^{-1} to 507 cm^{-1} as the aluminum content is increased (**Fig. 5.2.5**). This band grows in the relative intensity, which is characteristic of the presence of Al – O – Al bridges, with Al atoms tetrahedrally coordinated.
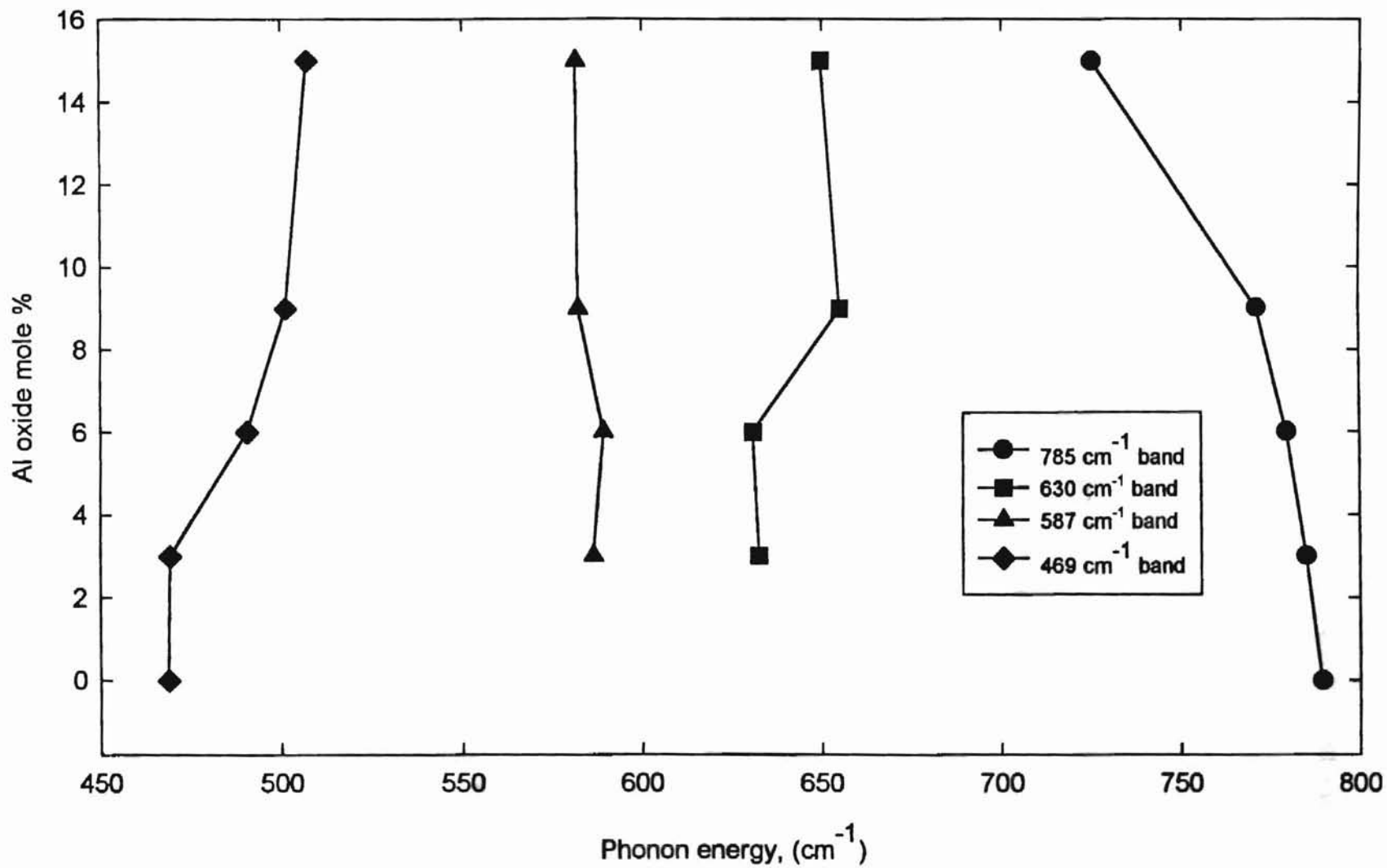
Fig. 5.2.5. Mid-frequency band positions vs Al oxide content

5.3. THE EFFECT OF SODIUM CONCENTRATION ON THE NETWORK OF EDSMAS GLASS.

Raman spectra of $[xNa_2O - 12MgO - 3Al_2O_3 - (85-x)SiO_2]_{97.5\%} - (Eu_2O_3)_{2.5\%}$ glasses have been taken with different content (x = 10%, 15%, 20%, 25%) of Na_2O (Fig. **5.3.1**). A similar deconvolution peak fit technique was applied to get detailed information on the vibrational structural properties of the glasses. A high frequency broad band was again peak fitted by three bands at 1096 cm^{-1}, 1012 cm^{-1} and 947 cm^{-1}, corresponding to the Q_3, Q_2 and Q_1 species respectively.

The position of the peak at **1096 cm^{-1}** shifts toward the lower frequencies from 1096 cm^{-1} to 1080 cm^{-1} as we increase the content of sodium atoms (**Fig. 5.3.2**). The width of the band is significantly reduced from 120 cm^{-1} to 94 cm^{-1} by sodium atoms (Fig. **5.3.3**). The position of the band at **947 cm^{-1}** shifts toward the higher frequencies from 947 cm^{-1} to 960 cm^{-1} as we increase the content of sodium atoms (**Fig. 5.3.2**). The width of this band broadens from its initial value 68 cm^{-1} to 90 cm^{-1} as the sodium content increases (Fig. **5.3.3**). The **1012 cm^{-1}** band slightly increases in frequency position to 1017 cm^{-1} as the sodium content goes up (**Fig. 5.3.2**). The width reduces from 97 cm^{-1} to 57 cm^{-1} (Fig. **5.3.3**).

From the first principles it is known that the alkalis are the network modifiers, they enter the glass as singly charged cations and occupy interstitial sites. The unit positive charge is satisfied by an ionic bond to an oxygen atom. This is accomplished by breaking a bridge and attaching an oxygen atom provided by the alkali oxide Na_2O to the broken bridge. Thus, each alkali ion is expected to create one NBO.
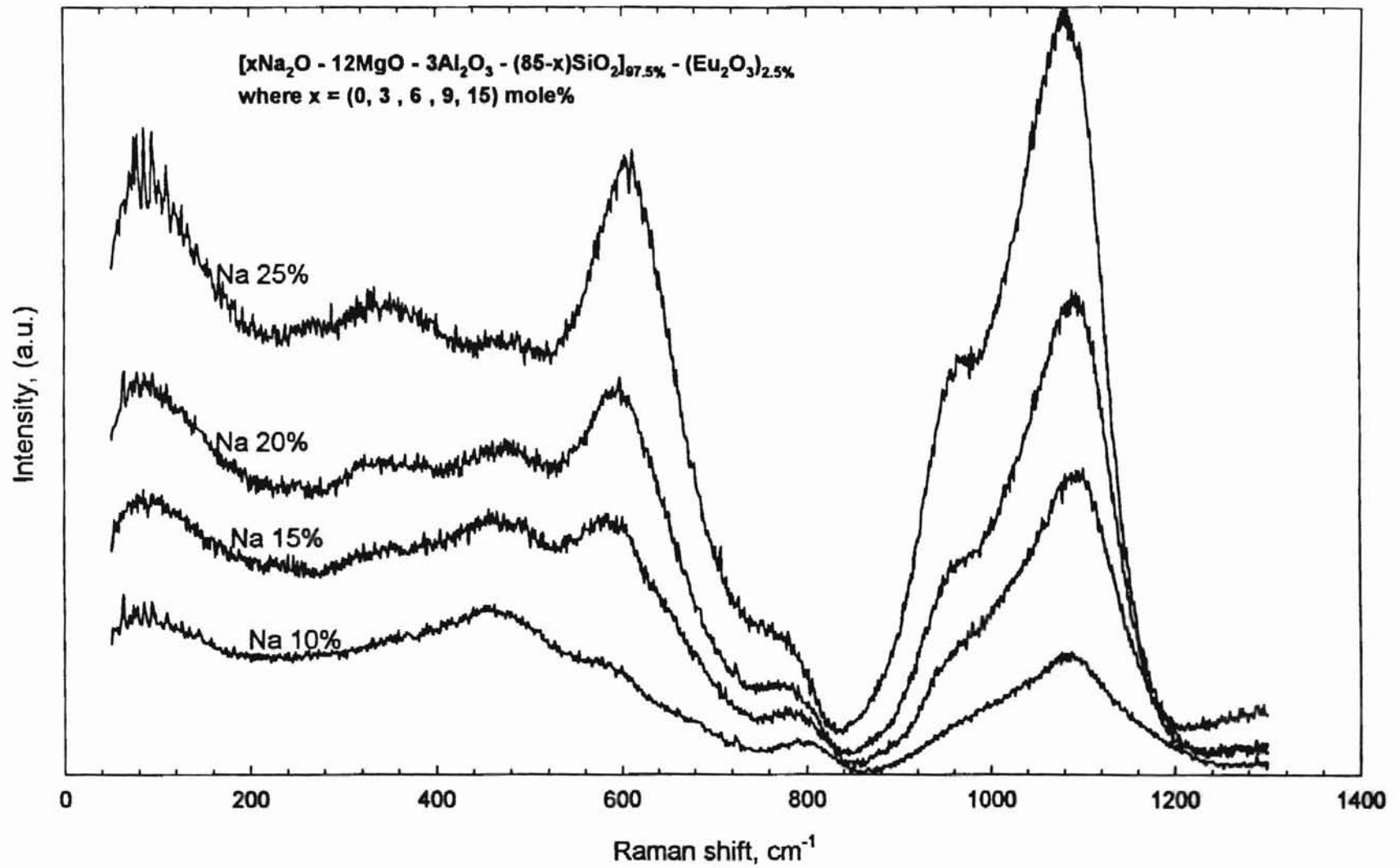
Fig. 5.3.1. Raman spectra of EDSMAS glasses for different Na content

$[xNa_2O - 12MgO - 3Al_2O_3 - (85-x)SiO_2]_{97.5\%} - (Eu_2O_3)_{2.5\%}$

where x = (0, 3 , 6 , 9, 15) mole%

Na 25%

Na 20%

Na 15%

Na 10%

Intensity, (a.u.)
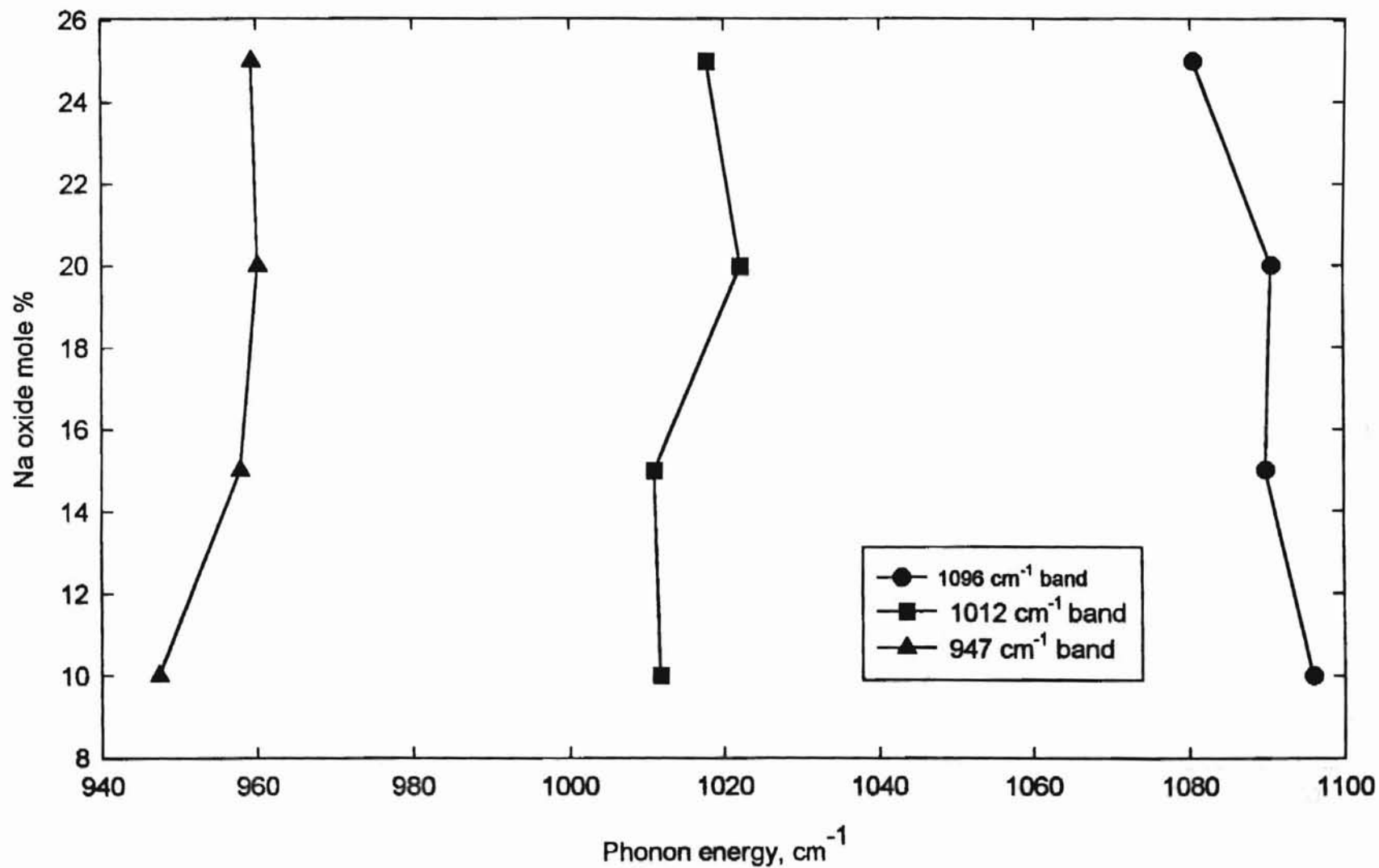
Raman shift, cm^{-1}

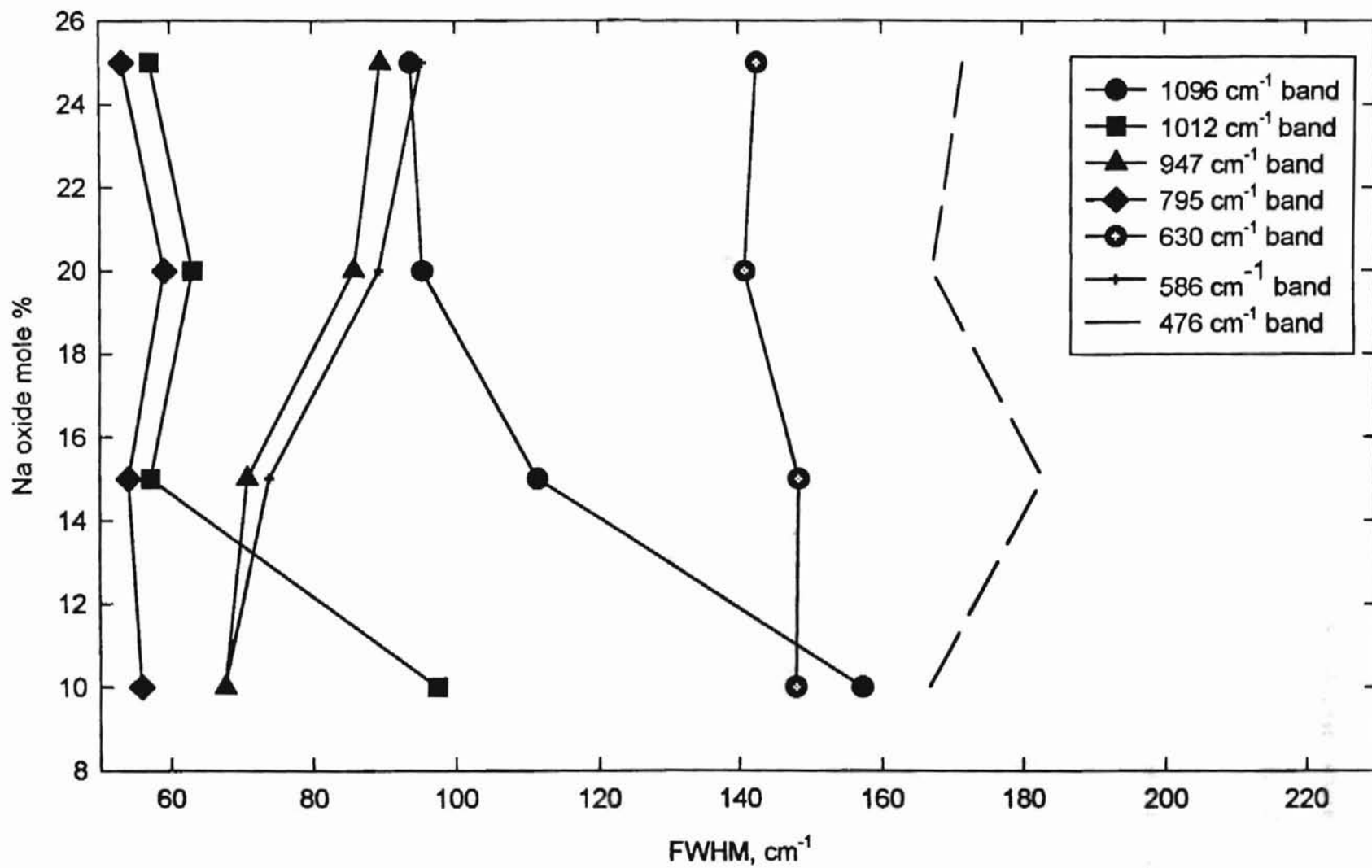Fig. 5.3.2. High frequency band positions vs. Na oxide content

Fig.5.3.3. FWHM of high- and mid- frequency bands vs. Na oxide content

Roughly speaking, this situation is opposite to the previous case where aluminum content was increased. However there are some peculiar features specifically inherent to sodium atoms. From the Raman data on our EDSMAS glasses, sodium atoms demonstrated the same modifying behavior. As the content of Na ions increases, the number of non-bridging oxygens grow which can be seen from the growth of the relative intensity of all high frequency bands (Q_1, Q_2 and Q_3 species) (see **Fig. 5.3.4 (a)**). This growth is also supported by the enhancement of the NBO ratio calculated according to Varshneya's approach (Fig. **5.3.4 (b)**). We believe that the growth of the number of NBOs is due to an increase in the number of ionically bound sodium ions with $Si - O - Na$ and $Al - O - Na$ bridges. Therefore, a decrease of weakly bound sodium ions which compensate charge of aluminum tetrahedra should also result. A schematic representation of strongly and weakly bound sodium ions for tetrahedrally coordinated aluminum atoms is shown in the **Fig. 5.3.5**. Thus, the increase of sodium content with respect to aluminum as well as with respect to the whole host in EDSMAS glasses leads to effective formation of more strongly bound sodium ions.

The position of the mid-frequency peak at **795 cm^{-1}** shifts from its initial position 795 cm^{-1} to 771 cm^{-1} as we increase the content of sodium atoms (**Fig. 5.3.6**). We have already established that the position of this band is sensitive to the number of silicon atoms being in the glass network. Since this band is characterized by Si atoms vibrations on oxygen tetrahedral "cage", then adding more sodium ions leads to overall decrease of number of silicon atoms which leads to frequency downshift. The bandwidth is not affected by adding sodium atoms (Fig. **5.3.3**).
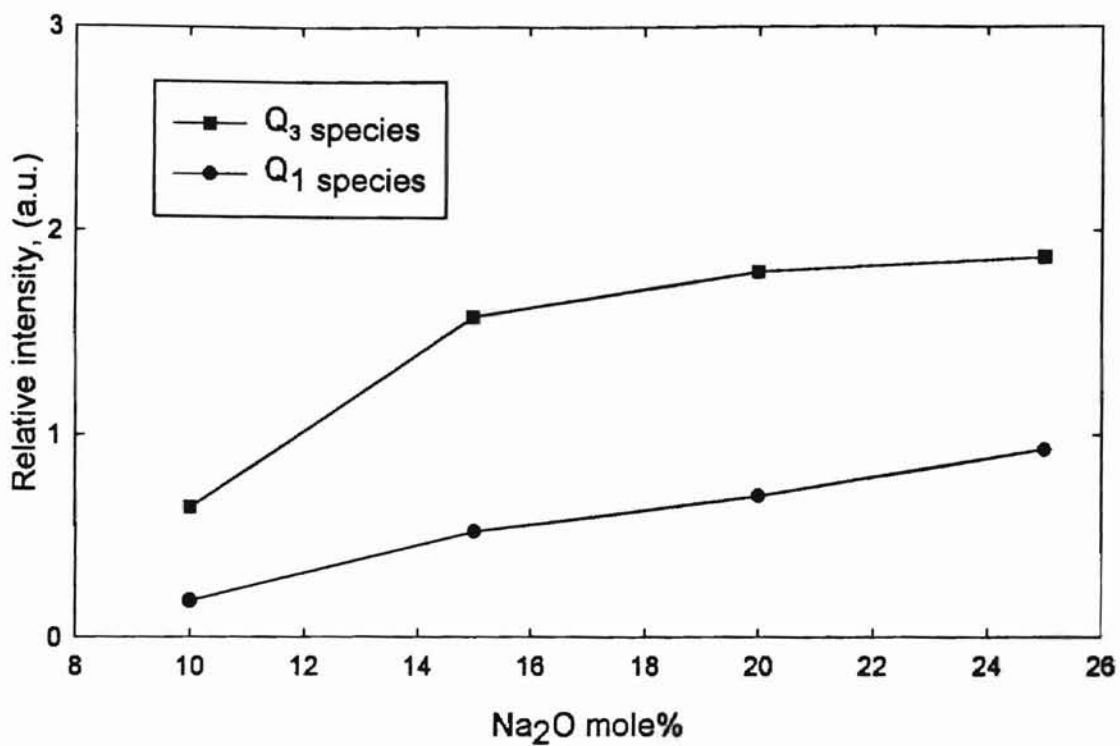
Fig. 5.3.4(a). The number of Q-species vs Na$_2$O content
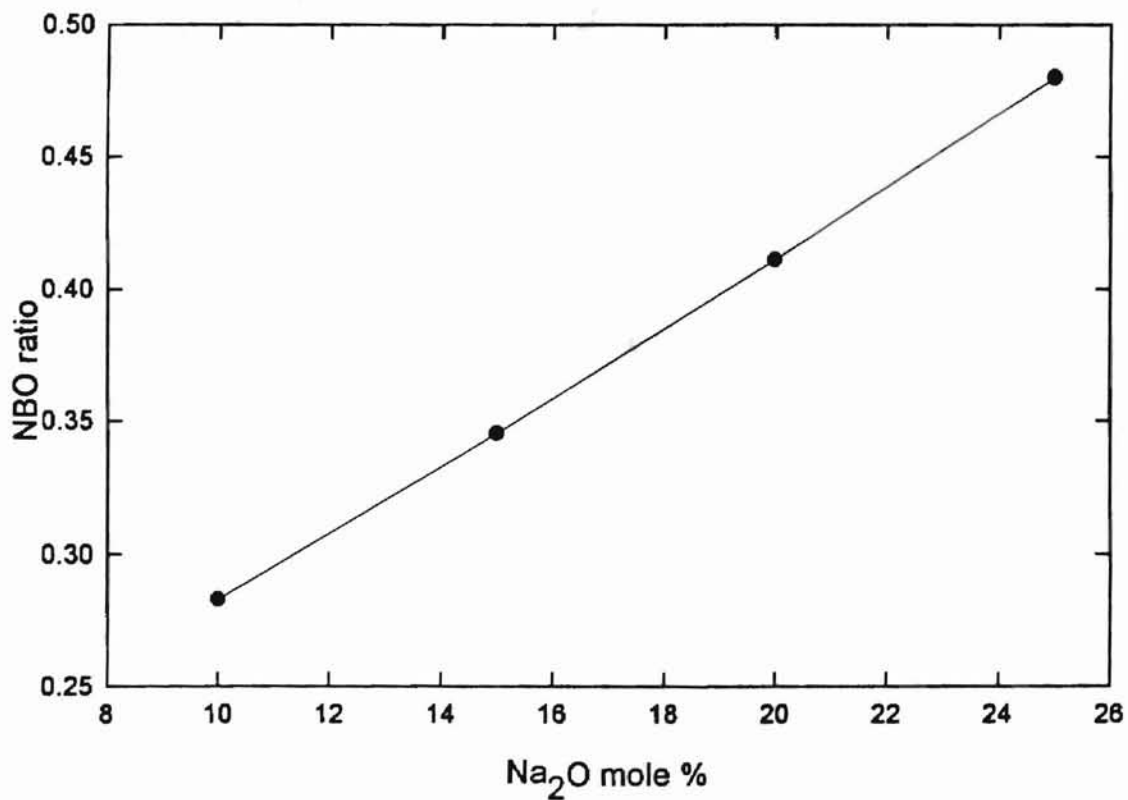
Fig. 5.3.4(b). Calculated NBO ratio vs. Na$_2$O content

Si
Al
O
Na

Na bound *strongly* to non-bridging O

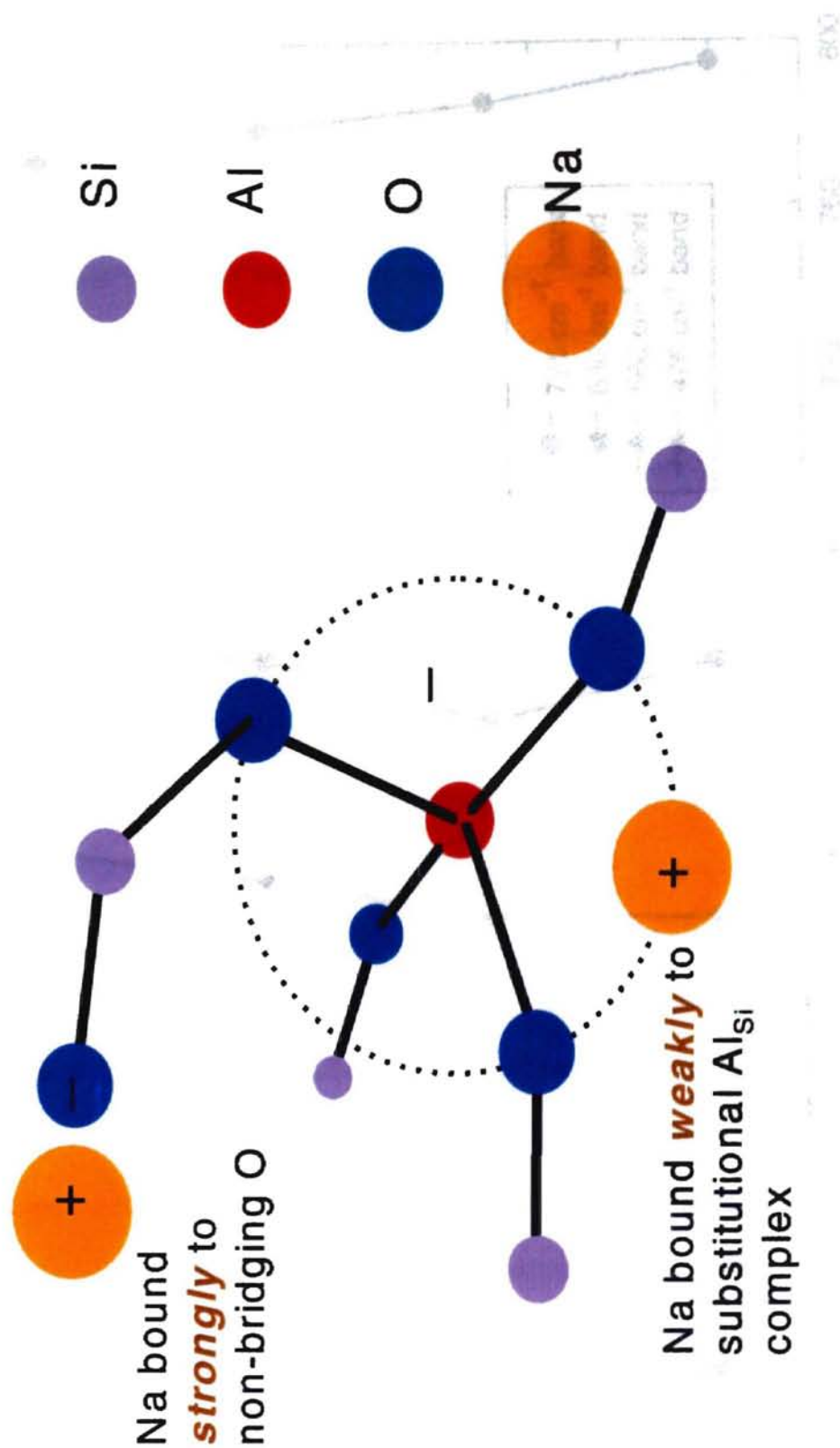Na bound *weakly* to substitutional Al_{Si} complex

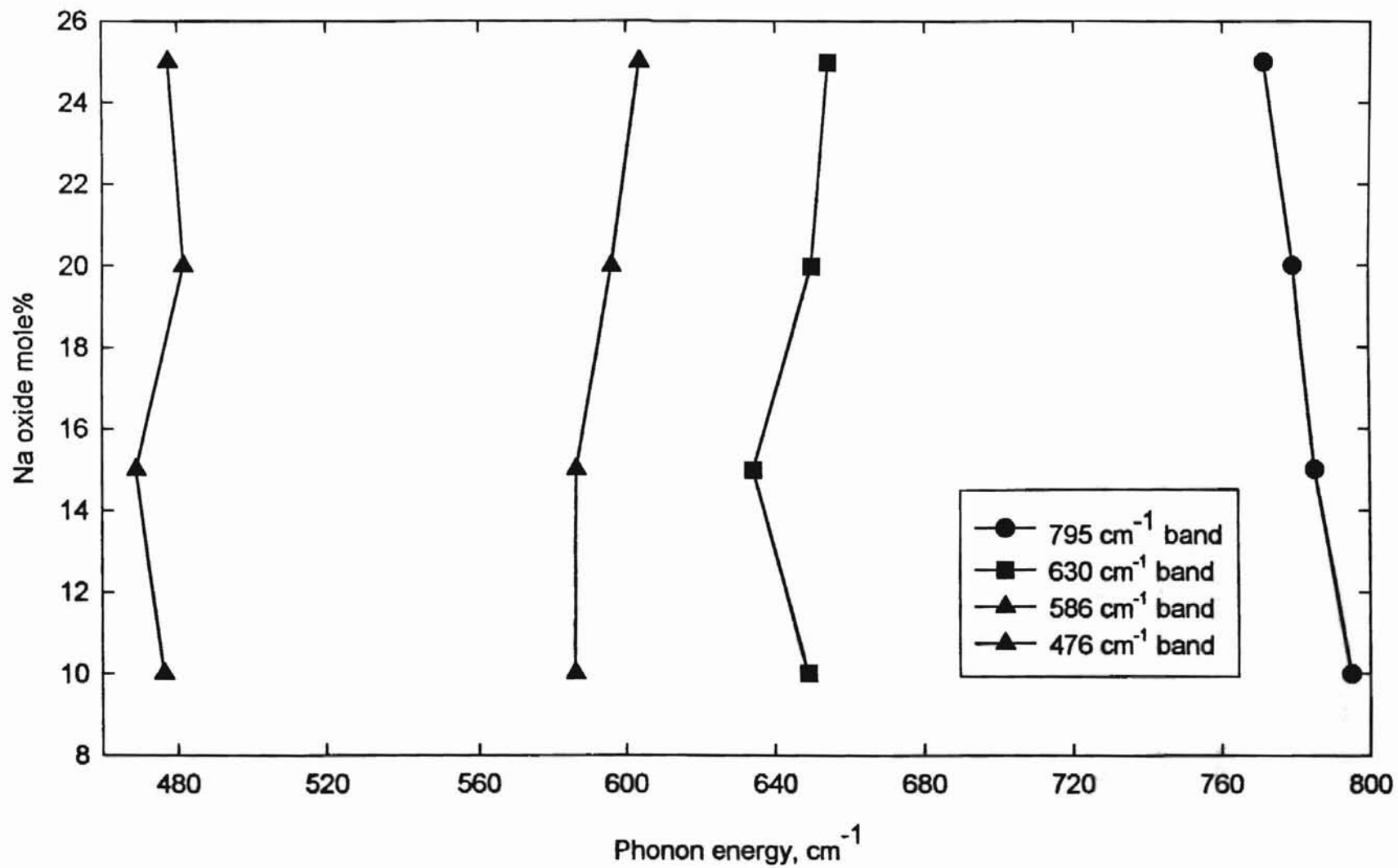**Fig. 5.3.5.** AlO_4 tetrahedral group

Fig. 5.3.6. Mid - frequency band positions vs. Na oxide content

The **633 cm^{-1}** shoulder gradually shifts toward the higher frequency from 633 cm^{-1} to 654 cm^{-1} as we increase the content of sodiums (Fig. **5.3.6**).

The **586 cm^{-1}** band in the previous section was assigned to the vibrations of Al – O – Si bridges with Al atoms tetrahedrally coordinated. Rapid growth of the band's relative intensity stands for the increase in number of these bridges associated with tetrahedrally coordinated aluminums, where sodium atoms compensate the charge of these tetrahedra (Fig. **5.3.5**). It is quite possible that some sodium atoms entering the glass cause Al^{3+} ions to form AlO$_4$-based complexes, so that, the increase of Al – O - Si bridges occurs. This is also supported by the fact, that the probability for the Al tetrahedron to be linked with silicon tetrahedron is much higher than that for Al tetrahedron to be linked with another Al tetrahedron because the number of Al atoms is significantly smaller that that of silicon atoms. Sodium ions compensating negative charge of aluminum tetrahedra become weakly bound.

The vibrational energy of this peak increased from 586 cm^{-1} to 604 cm^{-1} (**Fig. 5.3.6**). The bandwidth of this peak has been increased from 68 cm^{-1} to 95 cm^{-1} which is believed due to disrupting effect of sodium atoms entering the glass network.

The position and the width of **476 cm^{-1}** band are not sensitive to sodium content variations, however relatively high band intensity reduces as more sodium atoms are added. This happens most likely due to the decrease of the number of Al – O – Al bridges because some sodium atoms break these bridges and cause the formation Al-NBO vibrations .

New 350 cm^{-1} band appears due to incorporation of sodium atoms. Its shape becomes more pronounced as we increase the content of alkali atoms. We believe that

this band has been formed due to the enhancement of Eu − O − Na vibrations. Thus, sodium atoms modify low frequency vibrations mainly associated with Eu − O bridges. **Boson tail** has been also affected. Its relative intensity has been slightly increased due to incorporation of alkali atoms.

5.4. THE EFFECT OF POLARIZATION ON THE NETWORK OF [15Na$_2$0 − 12MgO − 3Al$_2$O$_3$ − (70-x)SiO$_2$]$_{97.5\%}$ - (Eu$_2$O$_3$)$_{2.5\%}$ GLASS.

We label VV when the scattered electric vector passed by the analyzer, E_{out}, is parallel to E_{in}; the spectrum is VH when $E_{Out} \perp E_{in}$. A purely isotropic scatterer would give no spectrum in VH configuration in electric dipole approximation. The result of polarization experiments of VV- and VH- Raman scattering on the [15Na$_2$0 − 12MgO − 3Al$_2$O$_3$ − 70SiO$_2$]$_{97.5\%}$ - (Eu$_2$O$_3$)$_{2.5\%}$ glass are shown on **Fig. 5.4.1(a)** and **5.4.1(b)** respectively. VH scattering reveals the presence of anisotropic scattering (i.e. contribution from off-diagonal elements in the Raman scattering tensor). The most pronounced effect of anisotropy in the structure of the glass can be seen in low frequency Boson tail. In those clusters where mid-frequency range of vibrations at 600 cm^{-1} take place, the structure is the most isotropic. This effect is consistent with the fact that mid-frequency broad band is highly polarized Raman peak as in vitreous silica.

Highly unpolarized nature of the band at 780 cm^{-1} is the manifestation of highest anisotropy in those clusters where Si atoms vibrations on oxygen tetrahedral "cage"
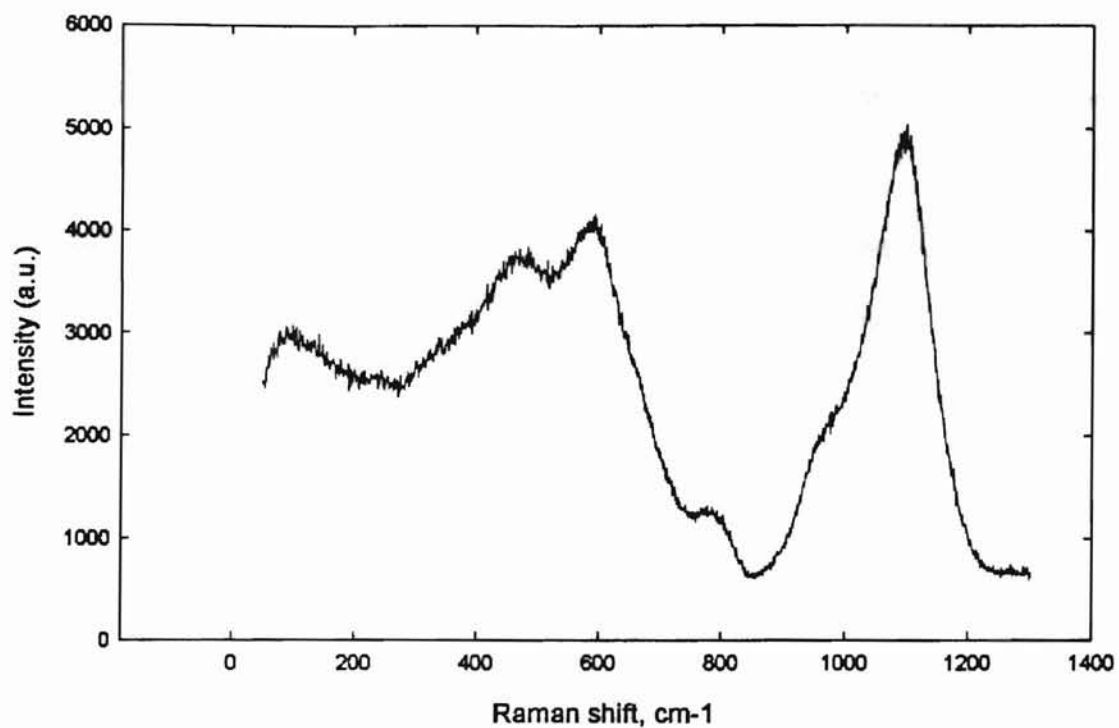
Fig. 5.4.1(a). VV - polarazied Raman spectrum of EDSMAS
glass with 2.5 mole % of Eu oxide
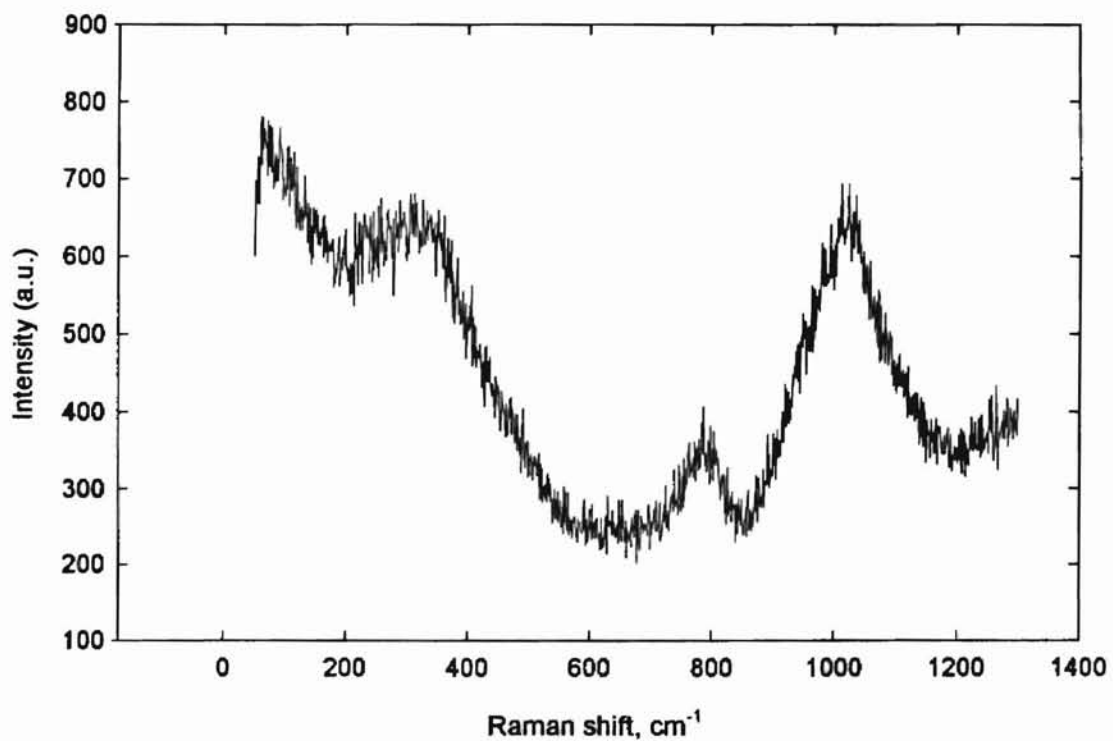
Fig. 5.4.1(b). VH - polarized Raman spectrum of EDSMAS
glass with 2.5 mole% of Eu oxide

occur, which is the obvious manifestation of fused silica's transverse optical mode associated with the "bond-bending" type of motion.

As far as the high frequency band is concerned, we can say that the isotropy plays an important role in tetrahedra having small numbers of non-bridging oxygens per tetrahedron since the 1100 cm^{-1} band is completely attenuated in relative intensity when we go from VV to VH type of polarization. However, tetrahedra having larger numbers of NBOs per tetrahedron are rather anisotropic.

CHAPTER VI

CONCLUSIONS AND SUGGESTIONS FOR FURTHER RESEARCH

Raman spectroscopic studies have been performed to investigate structural and vibrational properties of Eu^{3+} - doped soda magnesium aluminosilicate (EDSMAS) glasses as a function of content of individual components: Eu_2O_3 , Al_2O_3 and Na_2O to provide new knowledge related to the mechanism underlying the formation of holographic gratings in these glassy photorefractive materials during FWM experiment.

As was mentioned in Chapter 1, through the process of FWM experiment Eu^{3+} ions of EDSMAS glass are excited by the laser write beam to the off - resonance $^5D_2$ – energy level. Radiationless relaxation from this excited state to the $^5D_0$ metastable level results from the emission of several high-energy phonons on the order of 1000 cm^{-1} (Fig 1.2). This affects the structure of the glass modulating the index of refraction. In this sense, the role of high energy phonons ($\sim 1100\ cm^{-1}$) is believed to be crucial, since they fill the energy gap between the excited level and metastable $^5D_1$ as well as $^5D_0$ levels and provide the activation energy for some light modifiers (Na and Mg atoms) to migrate from the bright to dark region of the grating during FWM experiment, so that the permanent grating is formed.

We have studied phonon vibrations in EDSMAS glasses ranging from 50 cm^{-1} to 1300 cm^{-1}. Increasing the content of rare earth ions broadens the (800 – 1200) cm^{-1} band. This band also becomes more symmetric suggesting that the large variety of

different types of non-bridging oxygens (Q_1, Q_2 and Q_3 species) are available in EDSMAS glasses. From the growth of the relative intensities of the high frequency bands at 950 cm^{-1}, 1015 cm^{-1} and from the decrease of the relative intensity of 1100 cm^{-1} band, we deduced the overall growth of non-bridging oxygens (Fig. 5.1.5(a)). This is supported by a calculated increase in the NBO ratio (Fig. 5.1.5 (b)). In addition, it is known that high energy phonons associated with Si – NBO stretching vibrations are the most efficient in terms of filling the gap between excited and metastable levels of Eu^{3+} ions during nonradiative relaxation of europium ions in FWM experiment. These phonons are the most energetic ones in EDSMAS glass (Riseberg *et al*, (1968)). All these facts support experimental results of Hamad *et al* (Fig. 1.3) on the grating strength for various Eu_2O_3 concentrations.

At high content of Eu_2O_3 (> 10 mole %) the rate of FWM signal growth with Eu concentration is somewhat lower, which might be due to the simultaneous contributions of the following factors:

1) The appearance of low frequency vibrations associated with Eu – O and inter-tetrahedral vibrations. Low frequency phonons according to (Riseberg ET al., (1968)) are not very efficient in terms of coupling electronic and vibrational states. That is, low- energy phonons may play role of "friction force" for some modifiers to migrate, i.e. thermal resistance increases.

2) Thermal heating becomes pronounced due to absorption properties of Eu^{3+} ions. The more rare earth ions we excite the more heating of the local structure in the sample takes place. Broadening of the Raman bands takes place in Raman

scattering due to the same reason. This type of broadening is of phonon-phonon scattering nature. It is inversely proportional to the phonon lifetime.

3) Glass structure becomes saturated mostly by Q_2 and Q_1 species rather than Q_3 species which is seen from the Fig. 5.1.5(a) and from the frequency downshift of all three high frequency bands on the Fig. 5.1.4. That's why more weak "thermal generators" in the form of 1015 cm^{-1} and 965 cm^{-1} phonons contribute significantly rather than those in the form of 1100 cm^{-1} phonons.

It is necessary to note that at high concentrations Eu^{3+} ions might have different environments in the form of occupying different sites and having different bond lengths and angles and form higher order coordination spheres (**Fig. 6.1.**). There is always the possibility for the Eu^{3+} ions to cause the formation of some number of weakly bound sodiums necessary for compensating the charge of those high – order coordinated europiums at the expense of decreasing strongly bound sodiums. However this effect can't explain the slight attenuation in the FWM signal at high content of the rare earth ions simply because we don't know the effective contribution of strongly bound sodiums with respect to the contribution of weakly bound ones.

In the case of increasing the Al_2O_3 content we have seen that the EDSMAS glass gets fewer and fewer non-bridging oxygens (Fig. 5.2.4(a) and Fig. 5.2.4(b)) because Al atoms enter the glass at the expense of silicon atoms. The high frequency bands decrease in the relative intensity with the growth of Al content. To explain the steady growth of the FWM strength signal with increased Al concentration obtained by Hamad et al, (1998) we suggest that Al atoms in this case enter into our glass mostly with tetrahedral coordination (Fig. 5.3.5), so that there is increase of the number of
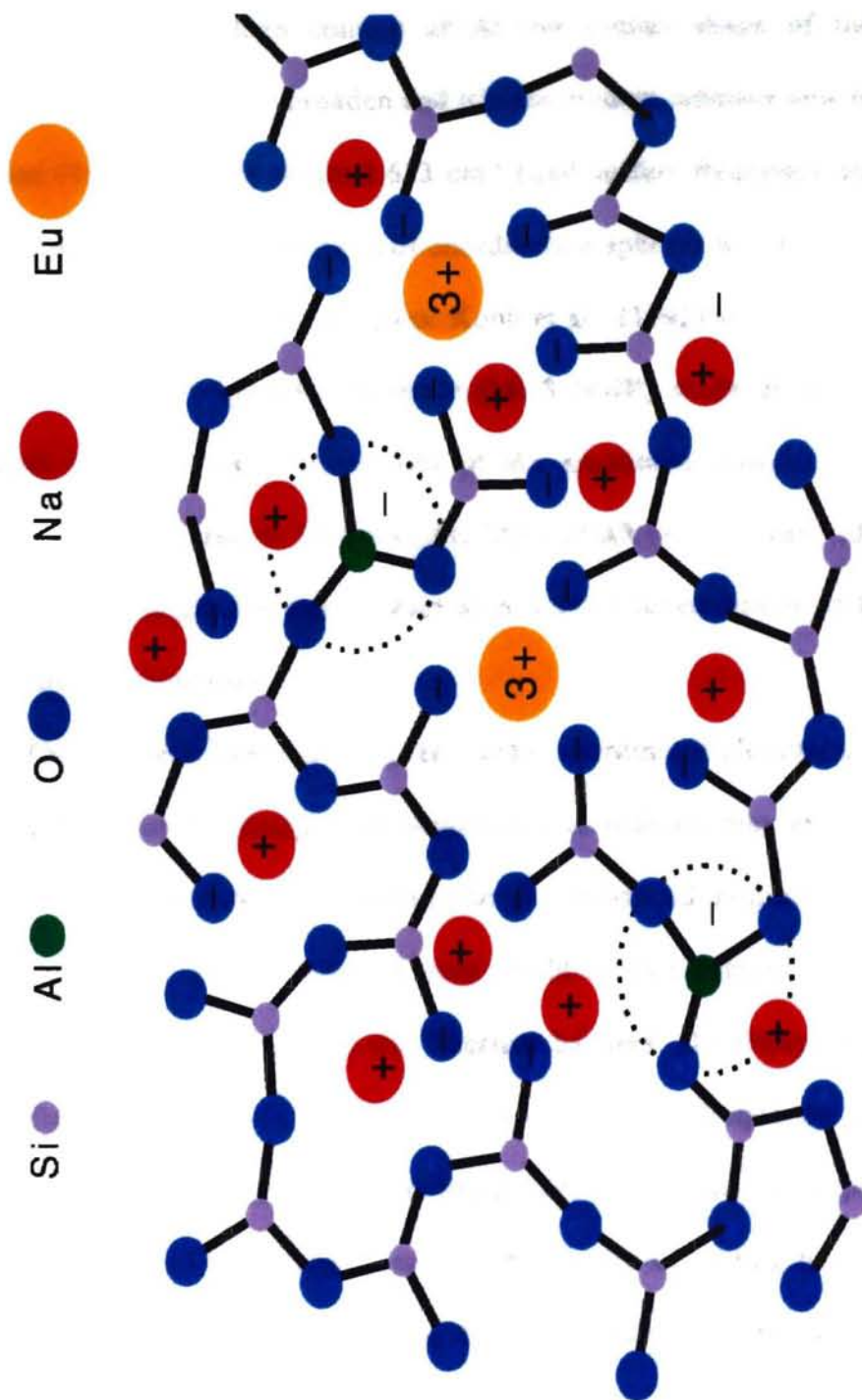
Fig.6.1. Schematic representation of Eu³⁺ ions environment

weakly bound sodiums at the expense of decrease of the number of strongly bound sodium atoms. At high content of Al the overall shape of the high- and mid-frequency bands start to broaden and it's not evident whether new bands appear in the region 700 cm^{-1} or the original 633 cm^{-1} band suffers frequency up-shift (Fig. 5.2.1). It is possible that the new types of coordination spheres will form due to high content of Al_2O_3 present in EDSMAS glass. Kohli et al., (1992) showed from the magic angle spinning nuclear magnetic resonance (MAS NMR) study of yttrium aluminosilicate glasses indicates that the majority of the aluminum ions in these glasses are in tetrahedral coordination. However, the MAS-NMR results clearly showed that yttrium aluminosilicate glasses also contain significant concentrations of five- and six- fold coordinated aluminum ions.

Thus, if the formation of higher – order coordinated aluminums is really possible, then the chance of getting more weakly bound sodiums may even increase. All these factors can significantly contribute to the enhanced migration of light modifiers (mostly sodium atoms) to travel from bright to dark regions of the grating through FWM experiment. However, the "thermal barriers" do always exist for these light modifiers to migrate in the form of inefficient mid-frequency phonons. From the Raman data we can suggest that these phonons become very pronounced at high concentrations of Al atoms. However, the chance of getting more and more weakly bound sodiums also grows. Thus, the small activation energy supplied by these inefficient phonons may provide mechanism for weakly bound sodiums to migrate through the grating. In addition, it is important to take into account the fact that when we increase the content of Al atoms, the concentration of Eu^{3+} ions is kept constant,

therefore, the absolute values of FWM strength signal as a function of Al ions is lower than those of FWM strength signal as function of Eu ions by about a factor of 2.

FWM experiment with different concentrations of sodium atoms with insignificant change in the concentrations of Al_2O_3 and MgO has already been done by A.Y. Hamad (1996). The decay in the rate of the FWM signal has been observed by him. From our Raman results on EDSMAS glass we can deduce the following facts. With an increase of sodium concentration the overall growth of Si – NBOs coordinated mostly to strongly bound sodium atoms takes place. That was observed from the growth of the relative intensity of $(800 - 1200)$ cm^{-1} bands. Thus, high-energy phonons get enhanced in their number. However, they provide activation energy to release strongly bound sodiums. At the same time the growth of the relative intensity of the 586 cm^{-1} band, assigned to the phonons characterized by the Al – O – Si bridge vibrations where Al atoms are tetrahedrally coordinated, also occurs. Sodium atoms responsible for the growth of this band are the weakly bound ions compensating negative charge of aluminum tetrahedra. Associated mid-frequency phonons are again not efficient in terms of filling the gap between excited and metastable levels of Eu^{3+} ions and their amount is not larger than that of high energy phonons which is seen from comparison of 586 cm^{-1} and $(800 - 1200)$ cm^{-1} bands relative intensities. Mid-frequency phonons may play role of "friction force" for some modifiers to migrate, i.e. thermal resistance could increase.

Above all, the thermal generation source in the form of excitation of europium ions is presumed to be constant since Eu_2O_3 content is kept permanent in these Raman measurements. Therefore, it is more likely that the four-wave mixing strength signal

will be decreased with enhancement of sodium concentration unless strong constant excitation rate of rare earth ions will be provided in the form of high content of europium atoms along with reduced content of fairly large strongly bound alkaline ions (magnesiums).

As a final note, it is necessary to take into consideration the competition between the number of effective high energy phonons needed to liberate strongly and weakly bound modifiers with the number of mid-frequency phonons to improve holographic grating formation in EDSMAS glasses.

The selection of optimum laser wavelength of excitation during the process of formation of permanent grating is also crucial to tailor the FWM data to that of Raman to achieve maximum favorable conditions.

As far as suggestions for further research, the logical supplements to the present research work would be the Raman spectroscopic studies along with FWM experiments on EDSMAS glasses with different Mg content as well as FWM experiment on EDSMAS glass with different Na content to confirm our predictions from Raman results. To get more information on the structural considerations in our glass alkaline modifier, neutron scattering and IR spectroscopes will be helpful. To obtain better understanding on the coordination types of Eu ions and Al atoms in EDSMAS glasses it is suggested to perform MAS-NMR as well as X-ray diffraction studies. To get more knowledge on the environment of Eu^{3+} ions it is necessary to do fluorescence measurements and to use fluorescence line narrowing technique.

Hopping of light modifiers such as Na and Mg atoms in our glasses during FWM experiment can be better understood by performing ionic conductivity measurements.

Low temperature Raman measurements along with Brillouin spectroscopy technique will give us new insights on the nature of acoustic vibrational modes as well as the Boson peak.

The main results of this work as far as Raman spectroscopic studies of EDSMAS glasses are concerned have been reported in recent APS Meeting (Utegulov, *et. al.*, 1999).

REFERENCES

Behrens et al., Applied Optics, Vol.29, No.11, 1990

Brawer S. and W. White, Journal of Chemical Physics, 63, No. 6, 1975

Brawer S.A. and W.B.White, J. of Non - Crystalline solids 23, p.261 – 278, 1977

Charles R. J., Journal of American Ceramic Society, 49 (1966) 55

Condrate R. A., Key Engineering Materials, Vol. 94-95, pp. 209 – 232, 1994

DeJong B. H. *et al.*, Geochim. Cosmochim. Acta 45 (1981) 1291

Dixon G. S., A.Y. Hamad and J.P. Wicksted, Phys. Rev B, Vol. 58, N.1, 1998

Durville F. M., Behrens E.G. and R.C. Powell, Phys Rev B, 35, 8, p.4109

Ellison A., Journal of Geophysical Research, vol.95, no. B10, pages 15,717 – 15,726

Furukawa T. *et al.*, Journal of Noncrystalline solids, 38/39, p. 87 – 92, 1980

Galeener F. L. and P.N. Sen, Phys. Rev. B 17, 1928 (1978)

Haller W., D. H. Blackburn and J. H. Simmons, Journal of American Ceramic Society, 57 (1974) 120

Hamad A.Y., PhD Thesis, 1996

Hamad A.Y., J. P. Wicksted, G. S. Dixon, C. A. Hunt and J. J. Martin "Effect of Eu^{3+} concentration on the grating efficiency in alkali-silicate glass", OSA meeting, Oct 4 – 9, 1998, Baltimore, Maryland, USA

Hamad A.Y., J. P. Wicksted, G. S. Dixon, C. A. Hunt and J. J. Martin "The influence of Al_2O_3 concentration on the grating kinetics in Eu^{3+} - doped alkali-silicate glass", OSA meeting, Oct 4 – 9, 1998, Baltimore, Maryland, USA

Kamitsos E. I. *et al.*, Journal of Non-Crystalline Solids 171 (1994), 31 – 45

Kohli J. T. *et al.*, Phys. Chem. of Glasses, 1992, 33 (3), 73 – 8

Kohli J.T., R.A. Condrate and J.E. Shelby, Physics and Chemistry of Glasses, Vol.34 No.3 June 1993

Kozuka H. *et al*, J. Mater. Sci. Lett., 1987, 6, 267

Krol D. M. *et al.*, Physics and Chemistry of Glasses, Vol.25, N 5, Oct 1984

Lee M. *et al.*, 1999 APS Meeting Bulletin, vol.2, p. 1662.

Matson *et al.*, Journal of non-crystalline solids 58 (1983) 323 – 352

McKeown D. A. *et al.*, Journal of Non-Crystalline Solids 68 (1984) 391 - 378

McMillan *et al.*, Journal of Non-Crystalline Solids, 53, 279 – 298, 1982

McMillan P., *et al.*, Geochim. Cosmochim. Acta 46 (1982) 2021

Merzbacher C. I. and W. B. White, American Mineralogist, Vol. 74, p. 1089, 1988

Mysen B.O. *et al*, Am. Mineral. 66, 678, (1981)

Mysen B. O. *et al.*, American Mineralogist, 67, p.686 – 695, 1982

Powell R.C. et al., Journal de Physique, Colloque C7, supplement 12, Tom 48, December 1987

Riseberg L. A., H. W. Moos, Phys Rev. 174, 429 (1968)

Sharma S. K, D.Virgo and B.O Mysen, American Mineralogist, 64 (1979) 779

Utegulov Zh.N., Hamad A.Y, Wicksted J.P., Dixon G.S., Martin J.J. "Raman Scattering Studies of the concentration dependence of Eu^{3+}- doped alkali modified

aluminosilicate glasses", APS 1999 Meeting Bulletin, March 20-26, Atlanta, Georgia, Vol.44, No.1, Part 2.

White W. B. in " Glasses for Electronic Applications", 1990

Varshneya A. K. "Fundamentals of inorganic glasses", 1994, Academic Press, Inc

Vita 2

Zhandos Utegulov

Candidate for the Degree of

Master of Science

Thesis: RAMAN SPECTROSCOPY STUDY OF RARE - EARTH DOPED
SILICATE GLASSES: MECHANISM UNDERLYING HOLOGRAPHIC
GRATING FORMATION

Major Field: Natural and Applied Sciences

Specialization: Physics / Photonics

Biographical:

Personal Data: Born in Almaty, Kazakstan, January 16, 1973, the son of Nurpeis
Utegulov and Iren Muldagalieva.

Education: Graduated from Kazakstan Physics and Math High School, Almaty,
Kazakstan, in June 1990; Received Honor Diploma in Physics (Bachelor
of Science, 6 year - program) in June 1996; completed the requirements
for Master of Science degree at Oklahoma State University in May, 1999.

Professional Experience: Research Assistant, Department of Physics, Kazak
State National University, Almaty, Kazakstan, August 1994 – June
1996; Teaching Assistant, Department of Physics, Oklahoma State
University, August 1996 to May 1997; Graduate Research Assistant,
Department of Physics, Oklahoma State University, May 1997 to present.

Professional Memberships: American Physical Society and Optical Society of
America